SPECTROSCOPIC, ELECTROCHEMICAL AND BIOLOGICAL STUDIES OF TRANSITION METAL COMPLEXES OF O - N - S DONOR LIGANDS

Thesis Submitted to the
COCHIN UNIVERSITY OF SCIENCE AND TECHNOLOGY
in partial fulfilment of the requirements for the degree of

DOCTOR OF PHILOSOPHY

in Chemistry

by

P. BINDU

DEPARTMENT OF APPLIED CHEMISTRY
COCHIN UNIVERSITY OF SCIENCE AND TECHNOLOGY
Kochi - 682 022, Kerala, INDIA

SEPTEMBER 1997

Dr. M.R. Prathapachandra Kurup
Reader
Department of Applied Chemistry
Cochin University of Science and Technology
Kochi 682 022
☎ 0484 - 555 804
Email chemist@md2.vsnl.net.in

CERTIFICATE

This is to certify that the thesis entitled **SPECTROSCOPIC, ELECTROCHEMICAL AND BIOLOGICAL STUDIES OF TRANSITION METAL COMPLEXES OF O-N-S DONOR LIGANDS** is an authentic record of the work done by Ms. P. Bindu, under my supervision in the Department of Applied Chemistry, Cochin University of Science and Technology and further that no part thereof has been presented before for the award of any other degree.

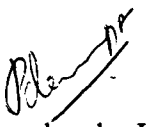

M.R. Prathapachandra Kurup
Supervising Teacher

Kochi 22
22nd September 1997

PREFACE

The work embodied in this thesis was carried out by the author in the Department of Applied Chemistry during 1994-'97. The primary aim of these investigations was to probe the spectroscopic, electrochemical and biological studies of some selected transition metal complexes of ^{4}N-monosubstituted thiosemicarbazones.

The chemistry of thiosemicarbazone complexes has received considerable attention recently, mainly due to their interesting physico-chemical properties, significant biological activities and analytical applications. The present study is confined to the spectroscopic, electrochemical and biological studies of copper(II), nickel(II), cobalt(II), and iron(III) complexes of ^{4}N-monosubstituted thiosemicarbazones.

Chapter I gives a brief survey about metal complexes of thiosemicarbazones, including their structural and bonding characterization, biological and analytical applications of transition metal complexes of thiosemicarbazones. Chapter II contains the synthesis of thiosemicarbazones and details regarding various characterization techniques. Chapter III to IV deal with the synthesis and characterization of copper(II), nickel(II), cobalt(II) and iron(III) ternary complexes of ^{4}N-monosubstituted thiosemicarbazones respectively. Electrochemical studies of copper(II) complexes and biological studies of copper(II) and nickel(II) complexes are also explored. Chapter VII includes the conductometric studies of manganese(II) complexes of acetone and butanone thiosemicarbazones in water at 283, 293, 303 and 313 K.

CONTENTS

CHAPTER I

METAL COMPLEXES OF THIOSEMICARBAZONES — A BRIEF SURVEY 1

1.1 Introduction 1

1.2 Bonding and Stereochemistry 1

1.3 Biological activity of thiosemicarbazones and their complexes 4

1.4 Objective and scope of the present work 5

CHAPTER II

SYNTHESIS, CHARACTERIZATION OF LIGANDS AND EXPERIMENTAL TECHNIQUES 7

2.1 Synthesis of ligands 7

2.2 Characterization of ligands 8

2.3 Analytical methods 13

2.4 Physico-chemical methods 13

CHAPTER III

SPECTRAL CHARACTERIZATION, CYCLIC VOLTAMMETRIC AND BIOLOGICAL STUDIES OF COPPER(II) COMPLEXES		**16**
3.1	Introduction	16
3.2	Experimental	17
3.2.1	Materials	17
3.2.2	Synthesis of complexes	17
3.2.3	Analytical methods	17
3.3	Results and discussion	17
3.3.1	Magnetic susceptibilities	20
3.3.2	Vibrational spectra	20
3.3.3	Electronic spectra	23
3.3.4	EPR spectra	26
3.3.5	Cyclic voltammetry	31
3.3.6	Biological activities	35

CHAPTER IV

SPECTRAL AND BIOLOGICAL STUDIES OF NICKEL(II) COMPLEXES		**38**
4.1	Introduction	38
4.2	Experimental	38
4.2.1	Materials	38
4.2.2	Synthesis of complexes	39
4.2.3	Analytical methods	39
4.3	Results and discussion	39

4.3.1 Magnetic susceptibilities 42
4.3.2 Vibrational spectra 42
4.3.3 Electronic spectra 45
4.3.4 NMR spectra 48
4.3.5 Biological activities 52

CHAPTER V

SPECTRAL CHARACTERIZATION OF COBALT(II) COMPLEXES 55
5.1 Introduction 55
5.2 Experimental 55
5.2.1 Materials 55
5.2.2 Synthesis of complexes 55
5.2.3 Analytical methods 56
5.3 Results and discussion 56
5.3.1 Magnetic susceptibilities 56
5.3.2 Vibrational spectra 59
5.3.3 Electronic spectra 59
5.3.4 EPR spectra 64

CHAPTER VI

SPECTRAL CHARACTERIZATION OF IRON(III) COMPLEX 66
6.1 Introduction 66
6.2 Experimental 66
6.2.1 Materials 66

6.2.2 Synthesis of complex 66
6.2.3 Analytical methods 67
6.3 Results and discussion 67
6.3.1 Magnetic susceptibility 67
6.3.2 Vibrational spectrum 68
6.3.3 Electronic spectrum 68
6.3.4 EPR spectrum 69
6.3.5 Mössbauer spectrum 72

CHAPTER VII

CONDUCTOMETRIC STUDY OF MANGANESE(II) COMPLEXES OF THIOSEMICARBAZONES AS A FUNCTION OF TEMPERATURE 75

7.1 Introduction 75
7.2 Experimental 76
7.2.1 Materials 76
7.2.2 Synthesis of complex 76
7.3 Results and discussion 76
7.3.1 Molar conductance 76
7.3.2 Effect of temperature 77
7.3.3 Dissociation constant 80
7.3.4 Activation parameters 80
7.3.5 Walden product 84
7.3.6 Limiting ionic conductance, ionic transport number and mobility 85

SUMMARY 87
REFERENCES 89
LIST OF PUBLICATIONS 100

ABBREVIATIONS

N_A	Avogadro number
C	Concentration
R_e	Corrected radius
R_{cr}	Crystallographic radius
ΔH_D	Change in enthalpy of dissociation
ΔH_{I-S}	Change in enthalpy of ion-solvent interaction
ΔG_D	Change in free energy of dissociation
ΔG_{I-S}	Change in free energy of ion-solvent interaction
ΔS_D	Change in entropy of dissociation
ΔS_{I-S}	Change in entropy of ion-solvent interaction
ΔE_p	Change in potential
ε	Dielectric constant
K_c	Dissociation constant
e	Electronic charge
E_a	Energy of activation
F	Faraday
E°	Formal potential
A	Frequency factor
R	Gas constant
λ_m	Molar conductance
λ°_m	Molar conductance at infinite dilution
m	medium (IR spectra)
s	strong (IR spectra)
sh	shoulder (Electronic spectra)
$\delta\varepsilon/\delta T$	Temperature coefficient
t_-	Transport number of anion
t_+	Transport number of cation
z_i	Valency of ion
η_o	Viscosity
vs	very strong (IR spectra)
w	weak (IR spectra)

CHAPTER I

METAL COMPLEXES OF THIOSEMICARBAZONES – A BRIEF SURVEY

1.1 INTRODUCTION

Metal complexes of thiosemicarbazones have been extensively studied and have been the subject of several reviews [1-4]. Thiosemicarbazones have been shown to exhibit wide range of biological activity which is thought to be related to their ability to chelate trace metals. In some instances transition metal complexes of thiosemicarbazones have been found to possess enhanced or modified activity in comparison to the uncomplexed ligands [4].

Thiosemicarbazones are obtained by condensation of thiosemicarbazides with suitable aldehydes or ketones. In solution thiosemicarbazones probably exist in an equilibrium mixture of thiol and thione tautomers.

1.2 BONDING AND STEREOCHEMISTRY

The stereochemistries adopted by thiosemicarbazone ligands while interacting with transition metal ions, depend essentially upon the presence of an additional coordination centre in the ligand moiety and the charge on the ligand, which in turn is influenced by the thione $\rightleftharpoons$ thiol equilibrium. It has been shown [5] that the arrangement of the non-hydrogen atoms in the thiosemicarbazide molecule is nearly planar and the sulfur atom and hydrazinic $^{2}NH_2$ group are *trans* with respect to the C–N bond. When forming complexes in this configuration bonding occurs *via* the sulfur atoms as a monodentate ligand. Gerbeleu *et al.* [6] have shown that coordination occurs through the hydrazido and imide nitrogens if the sulfur centre is substituted. However in most complexes [7], thiosemicarbazones coordinate as

bidentate ligands *via* the azomethine nitrogen and thione/thiol sulfur when an additional coordinating functionality is present in the proximity of the donating centres (e.g. 2-heterocyclic thiosemicarbazones) the ligands bond in a tridentate manner. This can be accomplished by either the neutral molecule [8] or by the monobasic anion upon loss of a hydrogen from ^{2}N [9]. There are instances reported, however, where the heterocyclic atom and the azomethine nitrogen are involved in bidentate coordination [10] and the sulfur atom is considered not to be coordinated, weakly coordinated to the same metal centre [11].

Besides the dentacity variation, consideration of the charge distribution is complicated in thiosemicarbazones due to the existence of thione and thiol tautomers. Although the thione form predominates in the solid state, solutions of thiosemicarbazone molecules show a mixture of both tautomers. As a result, depending upon the preparative conditions (particularly solvent and pH), the metal complexes can be cationic, neutral or anionic. Furthermore, it is possible to isolate complexes containing two inequivalent ligands--one protonated and one deprotonated--within the same metal complex [12, 13]. Ablov *et al.* [14] suggested that formation of these mixed "tautomer" complexes is promoted by trivalent central metal ions like Cr(III), Fe(III) and Co(III). It has been reported that 2,6-diacetylpyridine *bis*(thiosemicarbazone) [15] and ^{4}*N*-substituted 2,6-diacetylpyridine *bis*(thiosemicarbazones) [16] coordinate to the metal as pentadentate SNNNS donors and the complexes exhibit antitumour activity. Thiosemicarbazone ligands coordinate the metal centres as dianionic tetradentate SNON [17] and NNSS [18] have also been reported.

The *E* and *Z* isomers of 2-formylpyridine thiosemicarbazone [19] and other heterocyclic thiosemicarbazones [20] have been separated and characterized. The differentiation of stereochemistry between isomers was based upon the degree of deshielding observed for the ^{2}N proton of the *Z*-isomer. It has been reported that the *E*-isomer is the stable form of 2-acetylpyridine ^{4}*N*-methylthiosemicarbazone and, was not isomerised upon reflux over silica gel [21]. In contrast it has been

found [22] that when the ^4N atom of the thiosemicarbazone is incorporated in a ring, a mixture of three isomers exists. The third is the bifurcated *E*-hydrogen-bonded ring isomer.

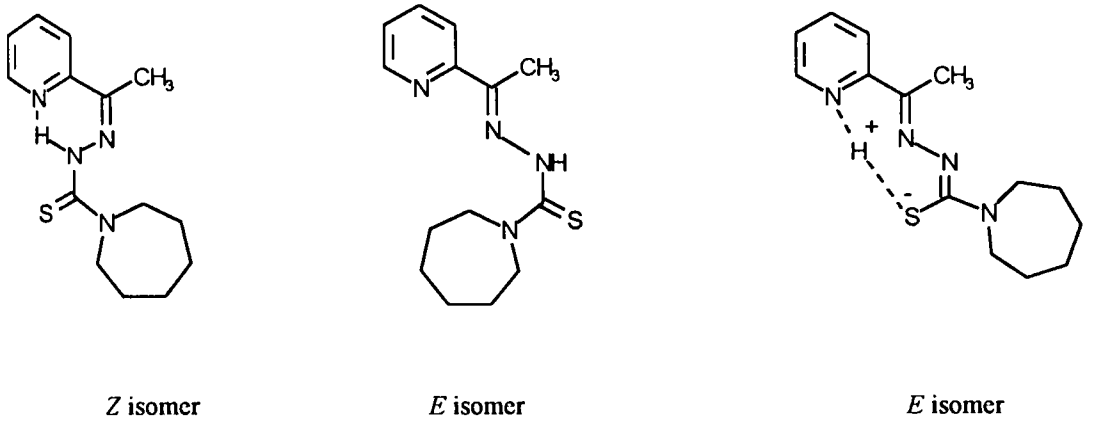

Z isomer *E* isomer *E* isomer

Figure 1.1 Isomers of 1H-hexahydroazepine-1-thiocarboxylic acid-2- [1- (2-pyridinyl)ethylidene]hydrazide in $CDCl_3$

Recent reports on spectroscopic and X-ray crystallographic study of 2-heterocyclic thiosemicarbazones [23 - 40] suggest that stereochemistries adopted by these complexes often depend upon the anion of the metal salt used and the nature of the ^4N-substituents.

Base adducts of copper(II) complexes of chelating agents formed by condensation of salicylaldehydes with *S*-alkyl esters of dithiocarbazoic acid [41], and thiosemicarbazones [42,43] have been reported. Base adducts of copper(II) and nickel(II) complexes of ONS ligands prepared from aldehyde/ketone and *S*-aryl/alkyldithiocarbazates have also been reported [44, 45]. Recently transition metal ternary complexes of glyoxalic acid thiosemicarbazone and 1,10-phenanthroline have been appeared in the literature [46], and an octahedral geometry is suggested for the complexes.

Thiosemicarbazones have been widely used as analytical reagents in the spectrophotometric determination of metals [47--50]. However, conductance studies of metal complexes of thiosemicarbazones have not been extensively studied [51, 52].

HSAB considerations dictate that the oxidation state of a metal affects the degree of its "softness" character, and this is found to be stronger for transition metals in low oxidation states. Thus the low spin d^8 ions Pd(II), Pt(II) and Au(III) and d^{10} ions Cu(I), Ag(I), Au(I) and Hg(II) exhibit higher stability constants with this class of sulfur ligands because of the formation of strong σ-bonds as well as dπ–dπ bonds by donation of a pair of electrons to ligands.

Of late preparation and X-ray crystal structure of the trimeric Cu(II) [53] and Ni(II) [54] complexes have been reported. In trimeric Cu(II) complex, the complex molecule contains a linear Cu_3 array in which the central copper atom at the crystallographic inversion centre has an octahedral environment and the other two Cu atoms are square pyramidal, each bridged to the central Cu atom *via* the ligand group. In trimeric Ni(II) complex aggregation was shown to proceed *via* Ni–O–Ni and Ni–S–Ni bridging, giving rise to both fourfold planar and pseudo-octahedral coordination of the nickel ions.

1.3 BIOLOGICAL ACTIVITY OF THIOSEMICARBAZONES AND THEIR COMPLEXES

The chemistry of thiosemicarbazone complexes has received considerable attention recently, mainly due to their significant biological activities. Thiosemicarbazones usually react as chelating ligands with transition metal ions by bonding through the S and hydrazinic N atom. The group >N-C=S is of considerable chemotherapeutic interest and is responsible for the pharmacological activity. It has been indicated that the microbial activity of these compounds is due

to their ability to chelate traces of metal ions. These findings have led increased interest in the chemistry of transition metal chelates of thiosemicarbazones.

Recently an excellent review about the structural and biological studies of thiosemicarbazone complexes of copper(II) have been appeared [55]. 2-Acetylpyridine ^4N-(2-acetoxyethoxymethyl)thiosemicarbazone was shown [56] to have, among a fairly large number of thiosemicarbazones, the highest inhibitory activity against the growth of the following microorganisms: *Staphylococcus aureus, Escherichia coli, Pseudomonas aeruginosa, Candida albicans* and *Aspergillus sp.* Isatine-β-thiosemicarbazones and methylisatin-β-thiosemicarbazones prevent the multiplication of small pox virus and the latter have also been used in the therapeutics of small pox [57]. Biological screening against a number of organisms has been carried out on many of these compounds and their uncoordinated thiosemicarbazones. There is a definite pattern in the biological activity and the size of the substituents attached to the thiosemicarbazone moiety among particular classes of thiosemicarbazones. Further, these complexes having thiol, rather than thione sulfur coordination, appear to be more active. Physico-chemical studies showed that lower g_{II} values, higher ν(d–d) band maxima and lower reduction potentials of their Cu(II) complexes are seemed to be related to increased biological activity.

1.4 OBJECTIVE AND SCOPE OF THE PRESENT WORK

Thiosemicarbazones have emerged as an important class of sulfur ligands [2,3] particularly for transition metal ions in the last two decades. The real impetus towards developing the coordination chemistry of these thiosemicarbazones has been provided by remarkable biological activities [4, 43, 55-57] observed for these compounds which has since been shown to be related to their metal complexing ability. The recent literature shows that this general class of compounds exhibits a wide range of stereochemistries on complexation with metal ions.

Thiosemicarbazones possessing antimalarial activity was first reported by Klayman *et al.* [58]. The influence on biological action have been studied by modifying the structure of 2-acetylpyridine thiosemicarbazone. (a) Exchange of sulfur atom of the thiocarbonyl group by oxygen, results in elimination of activity. (b) The point of attachment of the ethylidene moiety to the pyridine must be the 2-position and that attachment at the 3- and 4-positions eliminates activity. (c) The pyridine ring when replaced by phenyl, results in loss of activity.

In the light of these considerations it has been decided to prepare transition metal ternary complexes of salicylaldehyde ^{4}N-monosubstituted thiosemicarbazones with heterocyclic bases. Nearly forty complexes have been isolated and characterized by various physico-chemical methods. The complexes which included in this thesis are those of the transition metals Cu(II), Ni(II), Co(II) and Fe(III). Biological studies of Cu(II) and Ni(II) complexes have also been carried out. The last chapter gives a report about the conductometric study of *bis*(thiosemicarbazone)comploexes of manganese(II).

CHAPTER II

SYNTHESIS, CHARACTERIZATION OF LIGANDS AND EXPERIMENTAL TECHNIQUES

Details about the preparation of ligands and various analytical and physical methods employed in the characterization of metal complexes are presented in this chapter. Procedural details regarding the synthesis of metal complexes are given in appropriate chapters.

2.1 SYNTHESIS OF LIGANDS

The following ligands are used for the synthesis of complexes.

1. Salicylaldehyde ^4N-phenylthiosemicarbazone (H_2L^1)
i.e. [*N* - phenyl - 2 - [1 - (2 - hydroxybenzylidene] hydrazinecarbothioamide

2. Salicylaldehyde ^4N-cyclohexylthiosemicarbazone (H_2L^2)
i.e. [*N* - cyclohexyl - 2 - [1 - (2 - hydroxybenzylidene] hydrazinecarbothioamide

The two salicylaldehyde thiosemicarbazones have been synthesised by the following general method.

Aryl or alkyl isothiocyanate (100 mmol) was dissolved in 40 mL of ethanol and hydrazine hydrate (100 mmol) in 20 mL of ethanol was added slowly with constant stirring to the above solution. After the completion of the addition of hydrazine hydrate, the resulting solution was kept in stirred condition for 0.5 h. A white product formed was collected and washed subsequently with water and little ethanol and dried over P_4O_{10} *in vacuo*. The ^4N-monosubstituted thiosemicarbazides thus obtained were condensed with salicylaldehyde to get salicylaldehyde ^4N-monosubstituted thiosemicarbazones.

^4N-monosubstituted thiosemicarbazide (2 mmol) was dissolved in 25 mL of hot ethanol. To this hot solution, salicylaldehyde in ethanol (20 mL) was added with constant stirring, and the resulting solution was refluxed for 0.5 h. The pale yellow crystals separated were filtered, washed with 40% ethanol, recrystallised from ethanol and dried over P_4O_{10} *in vacuo*.

$$RNCS + H_2NNH_2 \longrightarrow H_2N\,NH\,C(S)\,NHR$$

$$H_2NNH\,C(S)\,NHR + C_6H_4(OH)\,CHO \longrightarrow C_6H_4(OH)\text{–}CH{=}N.NHC(S)NHR$$

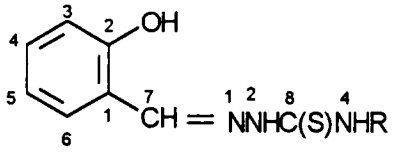

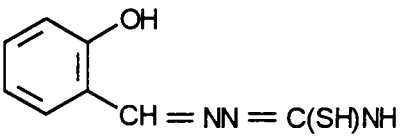

R = C_6H_5 or C_6H_{11}

Keto (thione) form

Enol (thiol) form

Figure 2.1 Tautomers of Salicylaldehyde thiosemicarbazone

2.2 CHARACTERIZATION OF LIGANDS

Salicylaldehyde ^4N-phenylthiosemicarbazone (H_2L^1)

mp 178° C

CHN : Found(Calcd.)% : C 61.87(61.97); H 4.70(4.82); N 15.35(15.49)

IR : ν(OH) 3150s; $\nu(^2NH)$ 3000m; $\nu(^7C{=}^1N)$ 1622s; $\nu(^2C\text{-}O)$ 1259s; ν(C=S) 1333s & 792m; $\nu(^1N\text{-}^2N)$ 1000m

^{1}H NMR: ^{1}H NMR spectrum is recorded in $CDCl_3$ - DMSO-d_6 mixture.

Signals at 11.36, 9.54 and 8.37 ppm are assigned to -OH, -^{2}NH and -^{7}CH=^{1}N protons respectively. H_2L^1 does not show any peak attributable to S-H proton, indicating that it exist in the thioketo form. Absence of -^{2}NH proton signal suggests enolisation of -^{2}NH-C=S group to -^{2}N=C-SH. The low field position of ^{4}NH (7.26 ppm) could be attributable to the deshielding caused by the phenyl group and the adjacent -N=C< of the system -N=C(SH)=NH-C_6H_5. Aromatic protons appear as multiplet at 6.84 -- 7.60 ppm range.

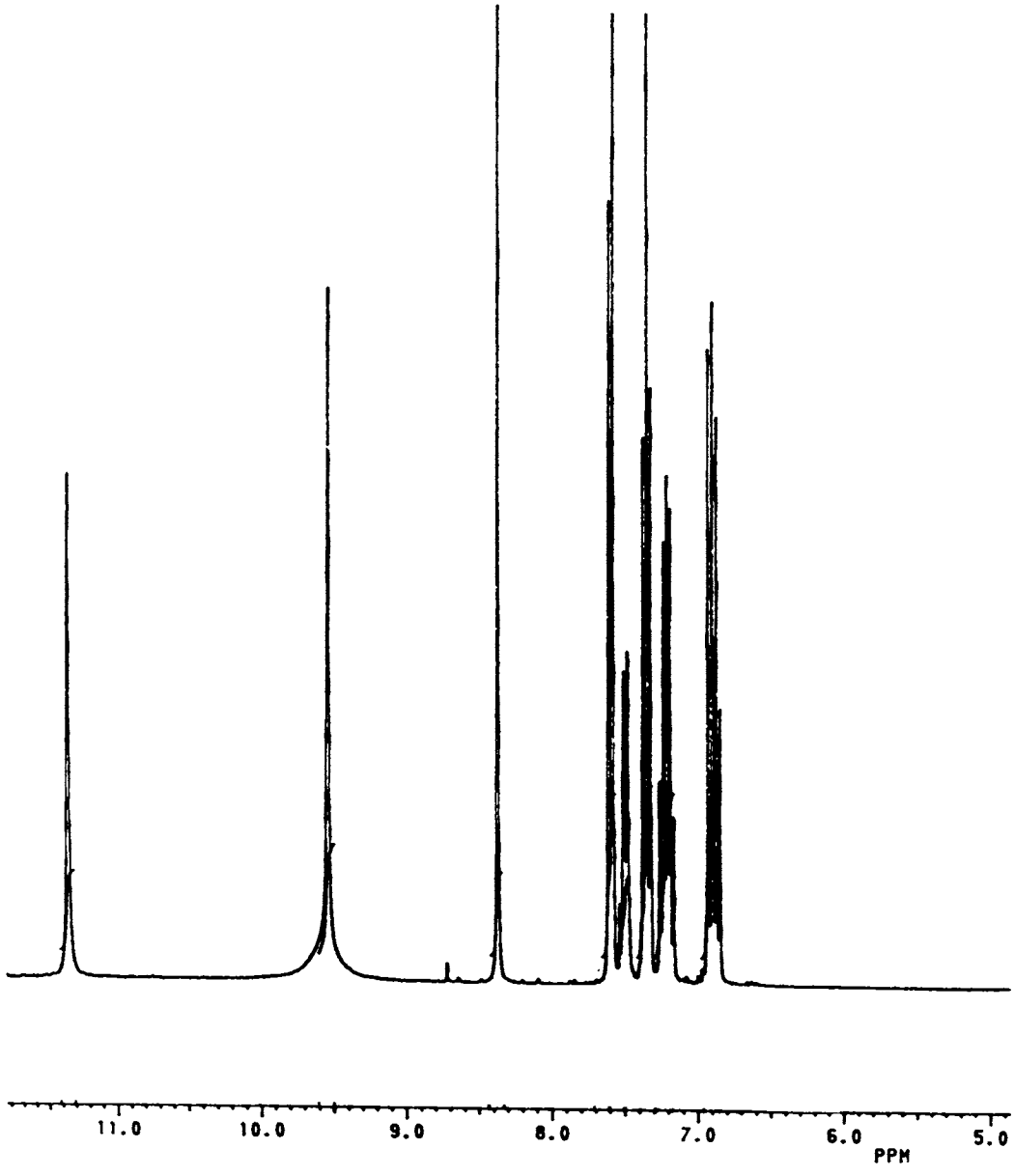

Figure 2.2 ^{1}H NMR spectrum of H_2L^1

^{13}C NMR : ^{13}C NMR spectrum is recorded in $CDCl_3$ - DMSO-d_6 mixture.

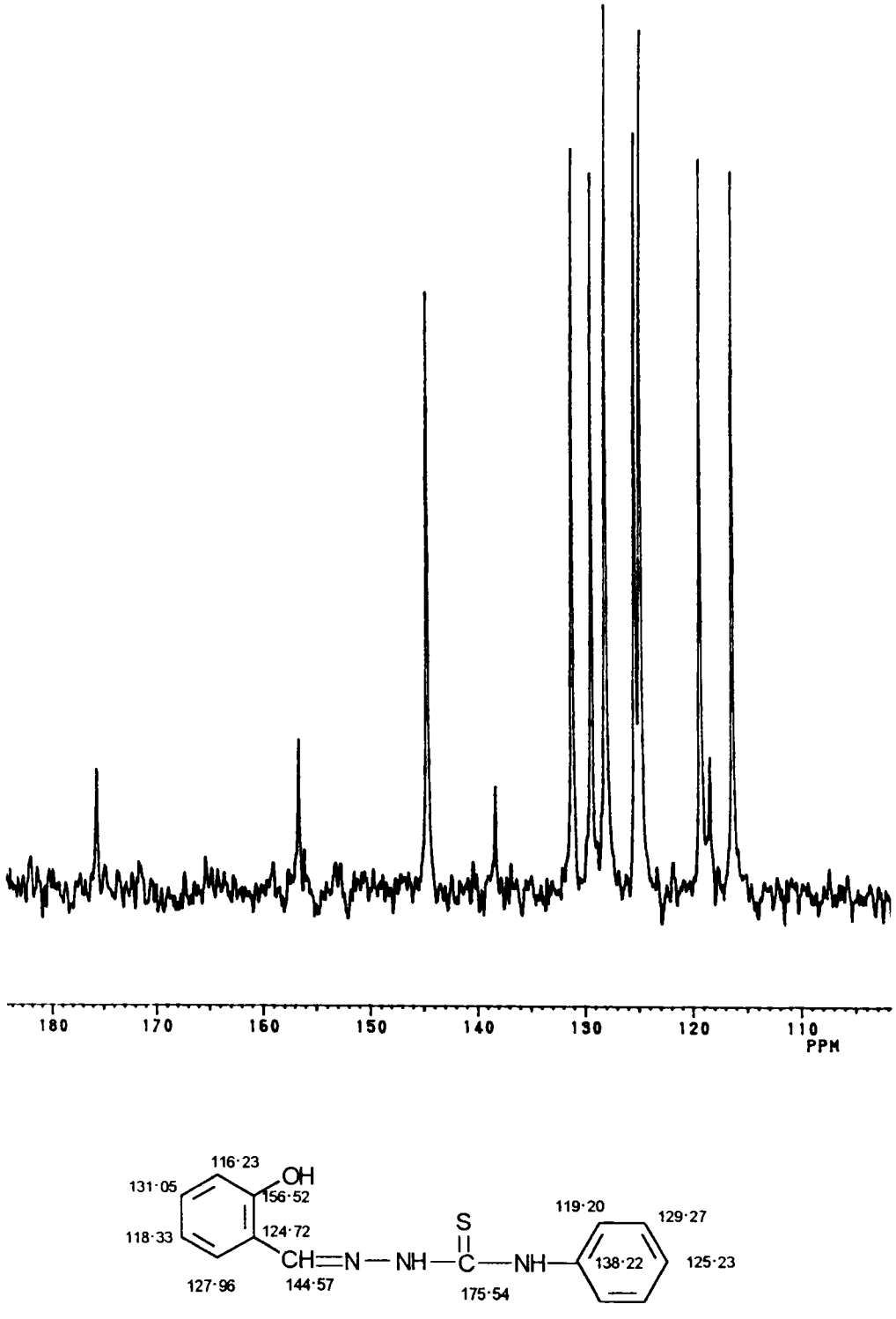

Figure 2.3 ^{13}C NMR assignments for H_2L^1

Salicylaldehyde ^4N-cyclohexylthiosemicarbazone (H_2L^2)

mp 184° C

CHN : Found (Calcd.) % : C 60.14(60.62); H 6.73(6.90); N 15.31(15.15)

IR : ν(OH) 3140s; ν(^{2}NH) 3250m; ν(^{7}C=^{1}N) 1620s; ν(^{2}C-O) 1269s; ν(C=S) 1335s & 860m; ν(^{1}N-^{2}N) 1016sh

^{1}H NMR: ^{1}H NMR spectrum is recorded in $CDCl_3$ - DMSO-d_6 mixture

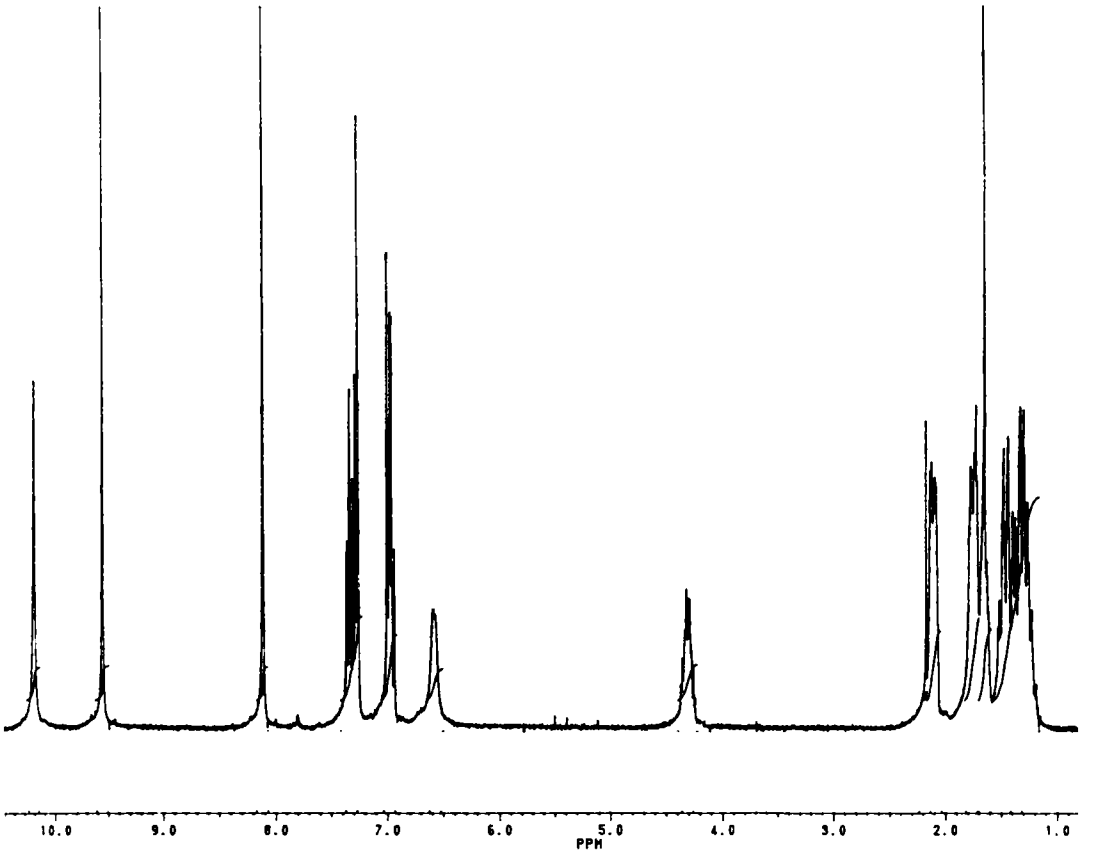

Figure 2.4 ^{1}H NMR spectrum of H_2L^2

Signals at 10.19, 9.55, 8.11 and 6.59 ppm correspond to -OH, -^{2}NH, -CH= and -^{4}NH protons respectively. The signal corresponds to S-H proton is absent.

Aromatic protons appear as multiplet at 7.25 -- 7.35 ppm range. Aliphatic protons appear at 1.18 -- 2.17 ppm range.

^{13}C NMR : ^{13}C NMR spectrum is recorded in $CDCl_3$ - DMSO-d_6 mixture.

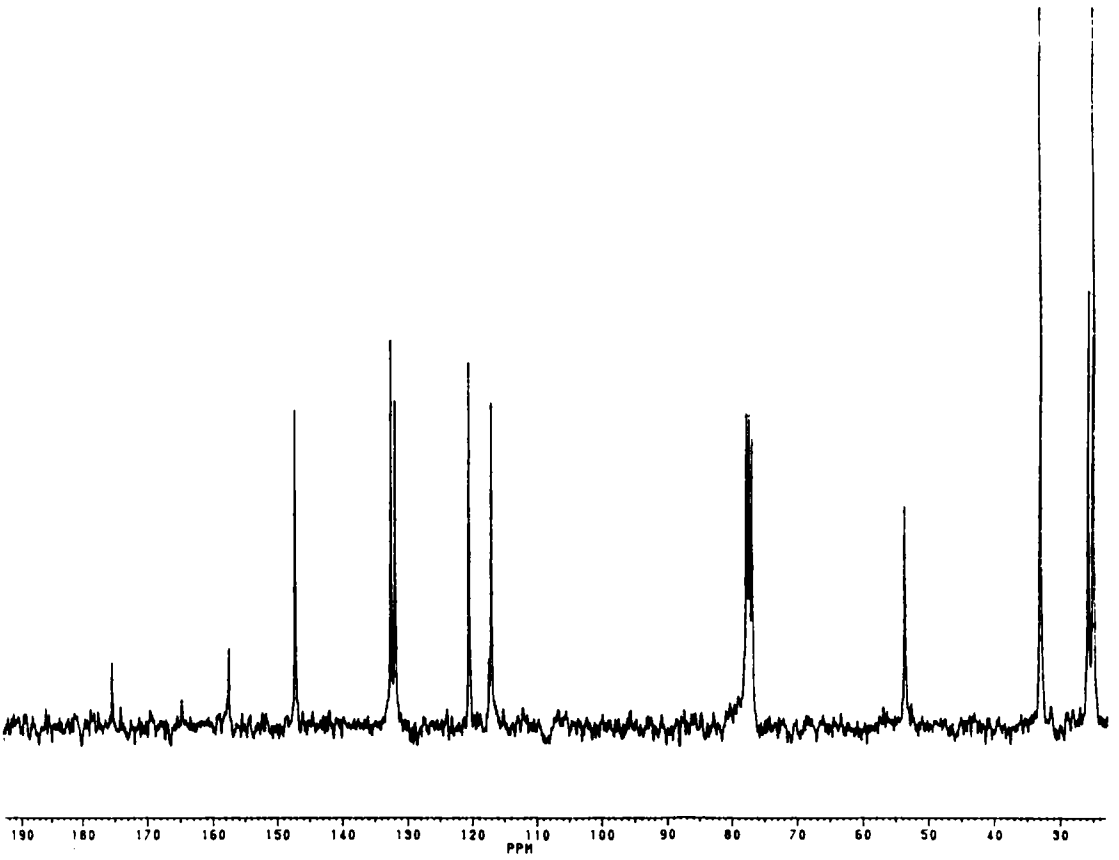

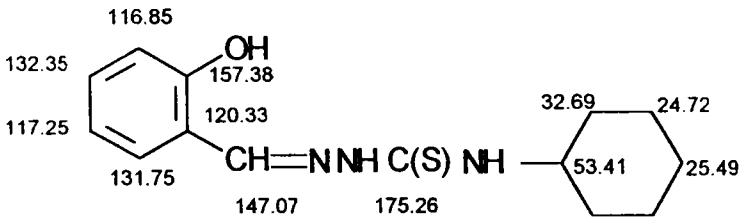

Figure 2.5 ^{13}C NMR assignments for H_2L^2

2.3 ANALYTICAL METHODS

Estimation of carbon, hydrogen and nitrogen

Microanalysis for carbon, hydrogen and nitrogen were done on a Perkin-Elmer Elemental Analyser at the RSIC, Panjab University, Chandigarh, India.

Estimation of metals

In all the cases the organic part of the metal complexes was completely eliminated by decomposition of the complexes in con. HNO_3, before the estimation of metals. Usual gravimetric procedures were used for the estimation of nickel, cobalt and iron. Copper was estimated by iodometric method.

2.4 PHYSICO-CHEMICAL METHODS

Magnetic susceptibility measurements

The magnetic susceptibility measurements were carried out at the USIC, University of Roorkee, Roorkee, India, in the polycrystalline state at room temperature on a Par model 155 Vibrating sample magnetometer at 5000 Oersted field strength. High purity nickel metal (saturation moment 55 emu/g) was used as a standard. Diamagnetic corrections were made by Pascal's constants.

Conductance measurements

Molar conductance of the complexes were measured in DMF (10^{-3} M solution) using a digital direct reading conductivity meter CM–180 Elico, Hyderabad. A calibrated dip type conductivity cell with platinised platinum electrodes (cell

constant 0.999 cm^{-1}) was used. The measurements were made at room temperature ±0.01° C.

Electronic spectra

Electronic spectra were recorded in DMF and Nujol mull on a Shimadzu model UV-Visible 160A spectrophotometer in the 200 – 1100 nm range.

Infrared spectra

IR spectra were recorded on a JASCO FT-IR-5300 spectrometer in the 4000 – 400 cm^{-1} range using KBr discs. Far IR spectra were recorded on a Bruker IFS 66V FT-IR spectrometer using polyethylene pellets over the 500 – 50 cm^{-1} range at the RSIC, IIT, Chennai, India.

NMR spectra

^{1}H and ^{13}C NMR spectra were recorded in $CDCl_3$ - DMSO-d_6 mixture on a Bruker AC- 300F NMR spectrometer (300 MHz) at the RSIC, Panjab University, Chandigarh, India.

EPR spectra

EPR spectra were recorded on a JEOL-FE 3X (X-band) spectrometer using diphenylpicrylhydrazide, (DPPH) (g = 2.0036) as calibrant at the University of Hyderabad, Hyderabad, India.

Mössbauer spectra

Mössbauer spectra were recorded on a Constant Velocity Mössbauer Spectrometer with a multichannel analyzer CMCA – 1000A supplied by M/s.

Wiessel Germany $^{57}Co(Rh)$ with 10 mci activity was used as the source, at the University of Madras, Gundy Campus, Chennai, India.

Cyclic voltammetry

Cyclic voltammetric studies were carried out on a Cypress System model CS - 1090/ model CS - 1087 computer controlled electroanalytical system. The three electrode system consisted of glassy carbon (working), platinum wire (counter) and Ag/AgCl (reference) electrodes at the University of Hyderabad, Hyderabad India.

CHAPTER III

SPECTRAL CHARACTERIZATION, CYCLIC VOLTAMMETRIC AND BIOLOGICAL STUDIES OF COPPER(II) COMPLEXES

3.1 INTRODUCTION

Investigations in coordination chemistry of copper(II) continue to be of interest in developing models for copper proteins and in understanding factors, which give rise to seemingly infinite variety of distortions from regular stereochemistry observed in copper(II) complexes [59, 60]. Generally Cu(II) forms octahedral complexes with the weakening of two axial bonds or square planar complexes. There is another possibility of five-coordinated environment around the Cu(II) complexes giving square pyramidal or trigonal bipyramidal structures in which one ligand is weaker at the axial position. Electron spin resonance spectroscopy is one of the most suitable techniques for studying the changes in molecular structure of paramagnetic complexes in solution.

Recently there has been considerable interest in the study of Cu(II) complexes of thiosemicarbazones, mainly due to their interesting physico-chemical properties [26, 31, 34, 36, 53, 61, 62] and significant biological activities [27, 28, 33, 37, 43]. The synthesis, spectral characterization, cyclic voltammetric and biological studies of four- and five-coordinate mixed ligand complexes of Cu(II) with salicylaldehyde ^{4}N-monosubstituted thiosemicarbazones and heterocyclic bases are included in this chapter.

3.2 EXPERIMENTAL

3.2.1 Materials

Details regarding the preparation and characterization of the ligands are given in Chapter II.

3.2.2 Synthesis of complexes

The mixed ligand complexes, CuL^1B and CuL^2B (where L^1 and L^2 are the dianion of salicylaldehyde ^4N-phenyl- and ^4N-cyclohexyl-thiosemicarbazones respectively. B is pyridine, piperidine, β/γ-picoline, 1,10-phenanthroline or 2,2'-dipyridyl) have been prepared by mixing 2 mmol of the appropriate heterocyclic base in MeOH to a hot solution of thiosemicarbazone (2 mmol) in MeOH (25 mL). To this was added a hot and filtered solution of $Cu(OAc)_2 \cdot H_2O$ (0.544 g, 2 mmol) in MeOH (30 mL) with constant stirring. The mixture was heated under reflux for 5-8 h and the volume is reduced to half. The complexes, which separated overnight as microcrystalline powders, were throughly washed with hot water, hot methanol, then ether and dried over P_4O_{10} *in vacuo.*

3.2.3 Analytical methods

Details regarding the analytical methods and other characterization techniques are given in Chapter II.

3.3 RESULTS AND DISCUSSION

The colours, elemental analyses, stoichiometries of H_2L^1, H_2L^2 and its complexes are presented in Tables 3.1 and 3.2 respectively. Both

Table 3.1 Colours, elemental analyses and magnetic susceptibilities of copper(II) complexes of salicylaldehyde ^4N-phenylthiosemicarbazone

Compound	Colour	Found (Calcd.) (%)				μ (B.M.)
		C	H	N	Cu	at 300 K
H_2L^1	Pale yellow	61.87 (61.97)	4.70 (4.82)	15.35 (15.49)	----	----
$CuL^1py{\cdot}3H_2O$	Brown	49.18 (49.07)	4.69 (4.76)	11.89 (12.05)	13.80 (13.66)	1.85
$CuL^1pip{\cdot}3H_2O$	Brown	48.09 (48.35)	5.79 (5.97)	12.00 (11.87)	13.80 (13.46)	1.87
$CuL^1\beta\text{-pic}{\cdot}3H_2O$	Brown	50.01 (50.04)	5.14 (5.04)	12.00 (11.67)	13.60 (13.23)	1.83
$CuL^1\gamma\text{-pic}{\cdot}3H_2O$	Brown	50.22 (50.04)	5.50 (5.04)	11.98 (11.67)	13.19 (13.23)	1.85
$CuL^1phen{\cdot}H_2O$	Dark green	59.02 (58.80)	3.59 (3.98)	13.30 (13.19)	11.59 (11.97)	2.01
CuL^1dipy	Dark green	59.20 (58.94)	3.80 (3.91)	14.28 (14.31)	13.20 (12.99)	1.92

Table 3.2 Colours, elemental analyses and magnetic susceptibilities of copper(II) complexes of salicylaldehyde ^4N-cyclohexylthiosemicarbazone.

Compound	Colour	Found (Calcd.) (%)				μ (B.M.)
		C	H	N	Cu	at 300K
H_2L^2	Pale yellow	60.14 (60.62)	6.73 (6.95)	15.31 (15.15)	---	---
$CuL^2py{\cdot}3H_2O$	Brown	48.54 (48.34)	5.87 (5.97)	11.90 (11.87)	13.53 (13.46)	1.85
$CuL^2pip{\cdot}2H_2O$	Brown	49.88 (49.60)	6.94 (7.01)	12.46 (12.18)	14.00 (13.81)	1.87
$CuL^2\beta\text{-pic}{\cdot}2H_2O$	Brown	51.70 (51.32)	6.21 (6.02)	12.00 (11.97)	13.72 (13.57)	1.88
$CuL^2\gamma\text{-pic}{\cdot}3H_2O$	Brown	49.13 (49.41)	6.02 (6.22)	11.68 (11.53)	13.12 (13.07)	1.89
$CuL^2phen{\cdot}H_2O$	Dark green	58.26 (58.14)	4.94 (5.06)	13.10 (13.04)	11.74 (11.83)	2.00
$CuL^2dipy{\cdot}2H_2O$	Dark green	54.42 (54.27)	5.38 (5.50)	12.99 (13.19)	11.90 (11.96)	1.95

thiosemicarbazones are pale yellow, while complexes prepared from py, pip, β/γ-pic are brown in colour. However the complexes prepared from phen and dipy are dark green in both series. Analytical data reveal the presence of one copper atom, one molecule of dianionic thiosemicarbazone and one molecule of heterocyclic base. The complexes are insoluble in most of the common polar and non-polar solvents. They are, however, soluble in DMF in which conductivity measurements were made, showing all complexes to be non-conductors [51].

3.3.1 Magnetic susceptibilities

The room temperature magnetic susceptibility of the complexes in the polycrystalline state fall in the 1.80 - 2.00 B.M. range, which are very close to the spin-only value of 1.73 B.M. for d^9. There is no magnetic evidence for any copper-copper interaction.

3.3.2 Vibrational spectra

The significant IR bands of H_2L^1, H_2L^2 and its copper(II) complexes are presented in Tables 3.3 and 3.4 respectively along with their tentative assignments. The absence of any band in the 2600 -- 2800 cm^{-1} region of the IR spectra of thiosemicarbazones suggests the presence of only thioketo form in the solid state [63]. On coordination of the azomethine nitrogen, $\nu[^7C=^1N]$ shifts to lower wavenumbers by 20 - 40 cm^{-1} [64], the band shifting from *ca.* 1620 cm^{-1} in the uncomplexed thiosemicarbazones' spectra to *ca.* 1595 cm^{-1} in the spectra of the complexes. Coordination of azomethine nitrogen is confirmed by the presence of a new band at 400 - 470 cm^{-1}, assignable to ν(CuN) for these complexes [26, 31, 34, 36]. The increase in ν(NN) in the spectra of complexes is due to the increase in double bond character off-setting the loss of electron density *via* donation of the metal and is a confirmation of the coordination of the ligand through the azomethine nitrogen atom. The spectral band $\nu(^2NH)$ of thiosemicarbazones disappears in the complexes indicating the deprotonation of the $-^2NH$ proton

Table 3 3 Infrared spectroscopic assignments (cm^{-1}) for the salicylaldehyde ^{4}N-phenyl-thiosemicarbazone and its copper(II) complexes

Compound	ν(CN)	ν(CO)	ν(NN)	ν(CS)	ν(CuN)	ν(CuO)	ν(CuS)	$\nu(CuN_{HB})$	Bands due to heterocyclic bases
H_2L^1	1622s	1259s	1000m	1333s 792m	----	---	---	---	---
$CuL^1py{\cdot}3H_2O$	1599s	1209s	1020w	1317s 746m	429s	391s	352s	332s	1250w, 620w, 440w
$CuL^1pip{\cdot}3H_2O$	1595s	1210s	1020w	1321m 744s	430s	391s	356s	336s	1100m, 588w
$CuL^1\beta\text{-pic}{\cdot}3H_2O$	1599s	1209s	1020w	1317s 746m	429s	391s	348s	331s	1250w, 610w, 450m
$CuL^1\gamma\text{-pic}{\cdot}3H_2O$	1599s	1209s	1020w	1317s 746m	429s	391s	352s	332s	1253m, 620w, 450w
$CuL^1phen{\cdot}H_2O$	1595s	1190s	1022sh	1315s 758m	466s	421s	388m	282m	1493s, 725s, 634m
CuL^1dipy	1595s	1244s	1012sh	1309s 767m	450s	413s	386m	243s	1469s, 1074m, 738m

Table 3.4 IR spectral assignments (cm^{-1}) for the salicylaldehyde ^{4}N-cyclohexylthiosemicarbazone and its copper(II) complexes

Compound	ν(CN)	ν(CO)	ν(CS)	ν(CuN)	ν(CuO)	ν(CuS)	$\nu(CuN_{H.B})$	Bands due to heterocyclic bases
H_2L^2	1620s	1269s	1335s 860m	---	---	---	---	---
$CuL^2py{\cdot}3H_2O$	1595vs	1201s	1277s 825s	410sh	392s	336s	309s	1250w, 633w, 450w
$CuL^2pip{\cdot}2H_2O$	1595vs	1201s	1277s 825s	413m	395s	337s	308s	1230w, 620m
$CuL^2\beta\text{-pic}{\cdot}2H_2O$	1597vs	1199s	1277s 825s	408s	393s	335s	310s	1250w, 615w, 450w
$CuL^2\gamma\text{-pic}{\cdot}3H_2O$	1597vs	1199s	1279s 826s	412s	393s	336s	310s	1258w, 655m, 450w
$CuL^2phen{\cdot}H_2O$	1601vs	1197s	1307s 846s	421s	387s	333s	322s	1467s, 727s, 510w
$CuL^2dipy{\cdot}2H_2O$	1595vs	1248s	1306s 827s	404s	385s	334s	315s	1439s, 1093s, 750w

and coordination *via* the thiolate sulfur is indicated by a decrease in the frequency (40 - 60 cm^{-1}) of the thioamide band which is partly ν(C=S) and found at 1333 and 792 for H_2L^1 and at 1335 and 860 cm^{-1} for H_2L^2 [65]. A shift to lower wavenumbers of these bands occur on complexation. The presence of a new band in the 330 - 380 cm^{-1} range assignable to ν(CuS) is another indication of the involvement of sulfur coordination. In H_2L^1 and H_2L^2 the ν(OH) band of salicylaldehyde appears at 3150 and 3135 cm^{-1} respectively. The phenolic oxygen on loss of the OH proton occupies the third coordination site, causing ν(CO) to shift to lower wavenumbers by 50 - 80 cm^{-1} from its position at 1259 and 1269 cm^{-1} in the spectra of H_2L^1 and H_2L^2 respectively. A new band in the 385 - 420 cm^{-1} range in the spectra of the complexes is assignable to ν(CuO). The fourth (and fifth) coordination site is occupied by the N-atom(s) of the heterocyclic base and we have assigned bands for ν(CuN) due to heterocyclic base in the 240 - 335 cm^{-1} range in the spectra of all the complexes. The IR spectra of the complexes display bands characteristic of coordinated heterocyclic bases [66 - 68].

3.3.3 Electronic spectra

The significant electronic absorption bands in the spectra of the complexes, recorded in DMF and Nujol mull are presented in Tables 3.5 and 3.6.

The thiosemicarbazones and copper(II) complexes have a ring $\pi \rightarrow \pi^*$ band at *ca.* 40,000 cm^{-1} and an $n \rightarrow \pi^*$ band at *ca.* 32,000 cm^{-1}, and little change in the energy of these bands occur on complexation. A second $n \rightarrow \pi^*$ band, located below 30,000 cm^{-1} in the spectra of uncomplexed thiosemicarbazones, is found at *ca.* 30,000 cm^{-1} in the spectra of copper(II) complexes. Two ligand-to-metal charge transfer bands are found at *ca.* 26,000 and 21,000 - 25,000 cm^{-1} range . In accordance with studies of previous copper(II) thiosemicarbazone complexes [69], the higher energy band is assignable to $S \rightarrow Cu^{II}$ transitions. The band in the 21,000 - 25,000 cm^{-1} range is assignable to phenoxy $O \rightarrow Cu^{II}$ transitions [70]. The d--d bands of copper(II) complexes, for

Table 3.5 Electronic spectral assignments (cm^{-1}) (log ε in parentheses)[a] for the salicylaldehyde ^4N-phenylthiosemicarbazone and its copper(II) complexes

Compound	Mode	d–d	L → M	n → π*	π → π*
H_2L^1	DMF	—	—	28,570sh (4.05) 32,380 (3.92)	39,063 (3.47)
	Mull	—	—	27,660, 32,484	40,625
$CuL^1py{\cdot}3H_2O$	DMF	17,515 (2.53)	24,690 (4.47) 25,240sh (4.48)	29,885sh (4.56) 33,900sh (4.46)	39,370 (4.17)
	Mull	16,925sh	24,075sh, 25,960sh	28,900, 32,925	42,370
$CuL^1pip{\cdot}3H_2O$	DMF	17,570sh (2.43)	24,630 (4.39) 25,245sh (4.41)	30,230sh (4.47) 34,015 (4.39)	39,215 (4.11)
	Mull	17,075sh	23,635sh, 25,380sh	28,890, 32,910sh	40,650sh
$CuL^1\beta\text{-}pic{\cdot}3H_2O$	DMF	17,685 (2.60)	24,690 (4.46) 25,245sh (4.47)	30,235sh (4.54) 33,900 (4.46)	42,620 (4.20)
	Mull	17,460sh	24,075sh, 26,180	29,030, 32,925	41,665
$CuL^1\gamma\text{-}pic{\cdot}3H_2O$	DMF	17,670 (2.58)	24,690 (4.48) 25,000sh (4.47)	30,235sh (4.57) 33,900 (4.48)	39,395 (4.17)
	Mull	17,745sh	24,075sh, 26,040	29,030, 32,930	42,370
$CuL^1phen{\cdot}H_2O$	DMF	17,795 (2.38) 13,685sh (3.84)	24,750 (4.33) 25,245sh (4.32)	30,230sh (4.44) 34,670sh (4.56)	39,460(4.23)
	Mull	18,330, 13,000sh	24,510, 26,805sh	29,885sh, 33,110	43,550sh
CuL^1dipy	DMF	17,670(2.41)	24,690(4.35) 25,240sh (4.37)	30,230sh (4.43) 35,210(4.57)	39,215(4.16)
	Mull	18,450, 128,20sh	24,300sh, 25,840		42,195

[a] ε are given in units of $dm^3\ mol^{-1}\ cm^{-1}$

Table 3.6 Electronic spectral assignments (cm^{-1}) (log ε in parentheses)[a] for the salicylaldehyde ^4N-cyclohexylthiosemicarbazone and its copper(II) complexes.

Compound	Mode	d–d	L → M	n → π*	π → π*
H_2L^2	DMF	—	—	25,525sh(4.00) 32,100sh(3.93)	39,215sh(3.57)
	Nujol	—	—	28,260sh, 31,325sh	41,270sh
$CuL^2py{\cdot}3H_2O$	DMF	17,670(2.61)	25,000(4.38) 26,000(4.35)	30,300(4.47) 34,485(4.37)	36,110sh(4.35) 39,215(4.00)
	Nujol	17,185sh	22,220sh, 25,975sh	28,820sh, 33,220sh	41,840
$CuL^2pip{\cdot}2H_2O$	DMF	17,600(2.57)	24,980(4.30) 26,000(4.27)	30,300(4.39) 34,845(4.29)	36,100sh(4.25) 39,065(3.84)
	Nujol	16,925sh	21,850sh, 26,000sh	28,570sh, 31,710sh	41,150
$CuL^2\beta\text{-}pic{\cdot}2H_2O$	DMF	17,605(2.65)	25,000(4.29) 26,000sh(4.26)	30,305(4.38) 34,720(4.28)	36,620sh(4.25) 38,910(3.81)
	Nujol	17,460sh	22,220sh, 26,000sh	28,960sh, 32,100sh	42,015
$CuL^2\gamma\text{-}pic{\cdot}3H_2O$	DMF	17,545(2.66)	25,000(4.34) 26,000sh(4.31)	30,305(4.42) 34,720(4.30)	37,680sh(4.25) 39,395sh(3.92)
	Nujol	17,185	22,035sh, 25,975sh	28,930sh, 31,710sh	41,840
$CuL^2phen{\cdot}H_2O$	DMF	13,885sh(2.09) 17,760(2.38)	24,875(4.20) 26,000sh(4.17)	30,490sh(4.29) 34,665sh(4.43)	37,175(4.60) 39,395sh(4.04)
	Nujol	12,965sh, 18835	24,075sh, 26,000sh	28,980sh, 32,100sh	38,325sh, 41,935sh
$CuL^2dipy{\cdot}2H_2O$	DMF	17,635(2.43)	24,060(4.22) 25,740sh(4.20)	30,300(4.31) 34,480(4.48)	36,110sh(4.42) 39,215(4.03)
	Nujol	12,800sh 18,450sh	23,245sh, 25,990sh	28,960sh, 31,955sh	37,040, 42,015

[a] ε are given in units of $dm^3\ mol^{-1}\ cm^{-1}$

which a square planar structure has been proposed, occur in the 16,000 - 20,000 cm^{-1} range [71, 72]. The solid state electronic spectra of CuL^1B and CuL^2B (B = phen, dipy) show d–d bands at *ca.* 12,800 and 18,400 cm^{-1} The spectra have no similarity to those shown by either square planar or octahedral copper(II) complexes of S–N ligands, but are similar to those shown by five-coordinate copper(II) complexes [73].

3.3.4 EPR spectra

The EPR parameters of copper(II) complexes obtained for the polycrystalline state (300 K) and in DMF (113 K) are presented in Tables 3.7 and 3.8.

The solid state EPR spectra also provide information about the coordination environment around Cu(II) in these complexes.

The spectra of some of the complexes recorded in the polycrystalline state at room temperature show typical axial spectra (Figure 3.1) while others show one broad signal (Figure 3.2), which is attributable to the dipolar broadening and enhanced spin-lattice relaxation [62] of the coordinating ligand. The four-coordinate complexes in frozen DMF show well resolved four copper hyperfine lines, characteristic of monomeric copper(II) complexes and nine superhyperfine lines (lines overlapped in some cases) (Figure 3.3) due to azomethine nitrogen and nitrogen atom of the coordinated heterocyclic base. Since superhyperfine coupling by a second nitrogen (nitrogen of the heterocyclic base) is observed, the coordinated heterocyclic base appears to be coplanar [74] with the ONS bichelate rings. So a square planar structure is assigned for CuL^1B and CuL^2B (B = py, pip, and β/γ-pic) complexes.

The EPR spectra of five-coordinate Cu(II) complexes in frozen DMF show that the expected superhyperfine splitting of three nitrogen atoms (one azomethine nitrogen and two nitrogens from phen or dipy) are not observed

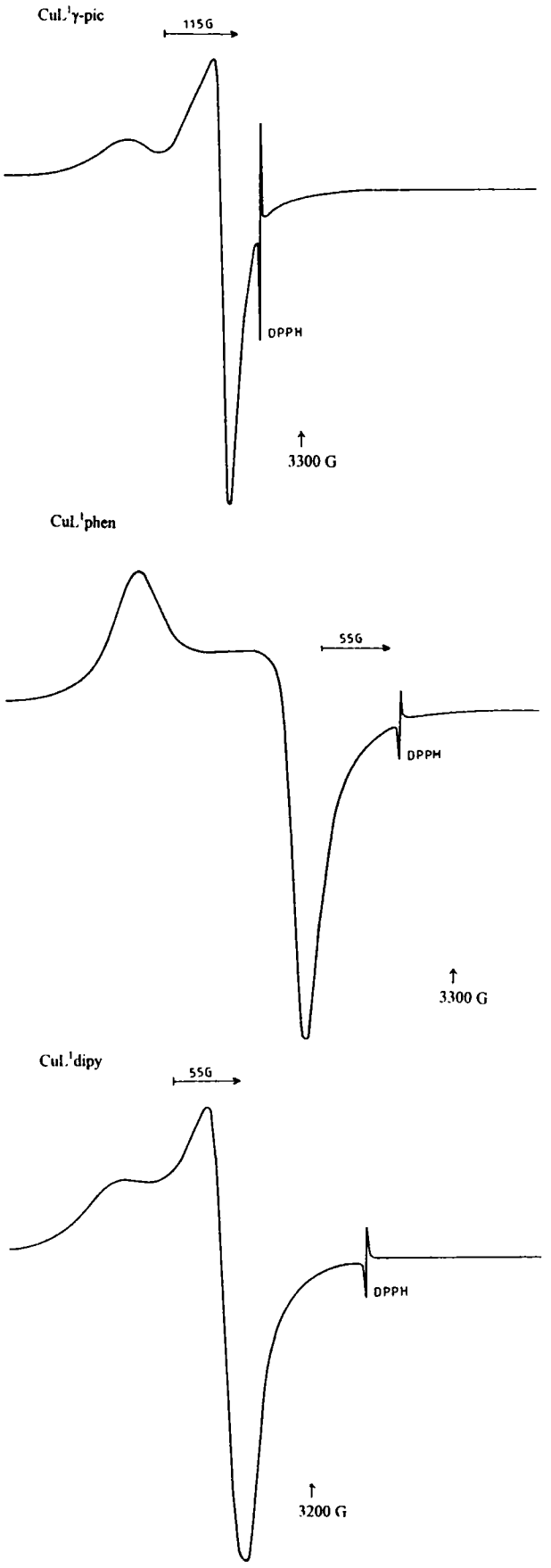

Figure 3.1 EPR spectra of Cu(II) complexes in polycrystalline state at 300 K

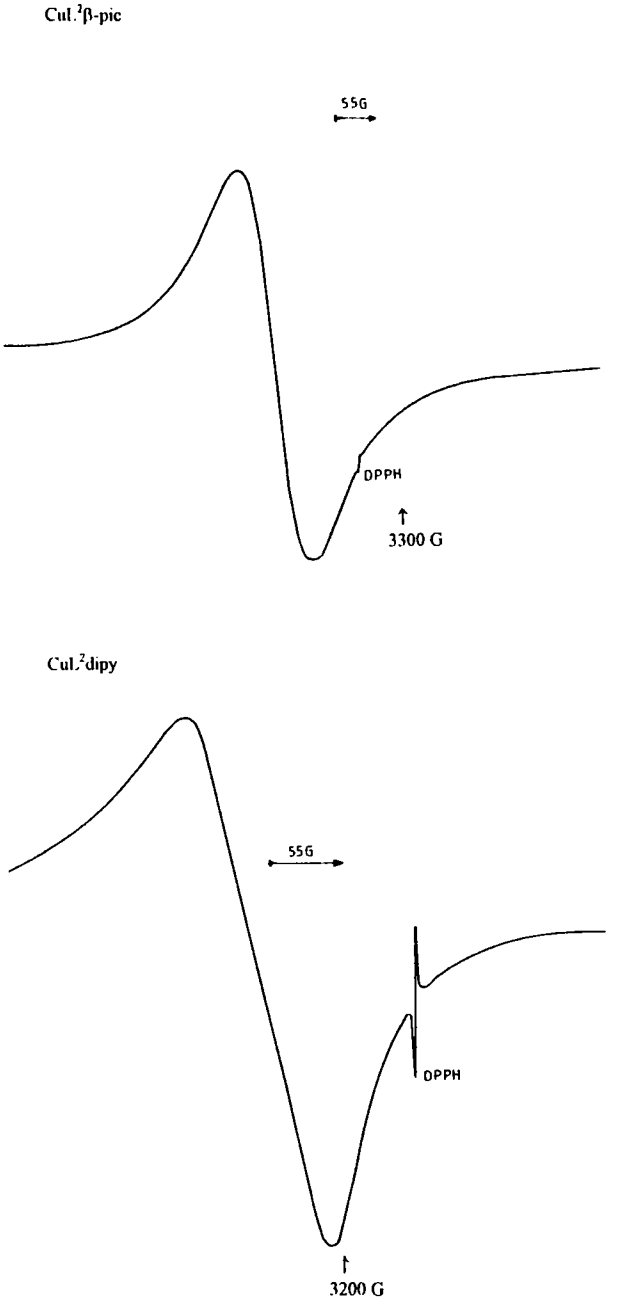

Figure 3.2 EPR spectra of Cu(II) complexes in polycrystalline state at 300 K

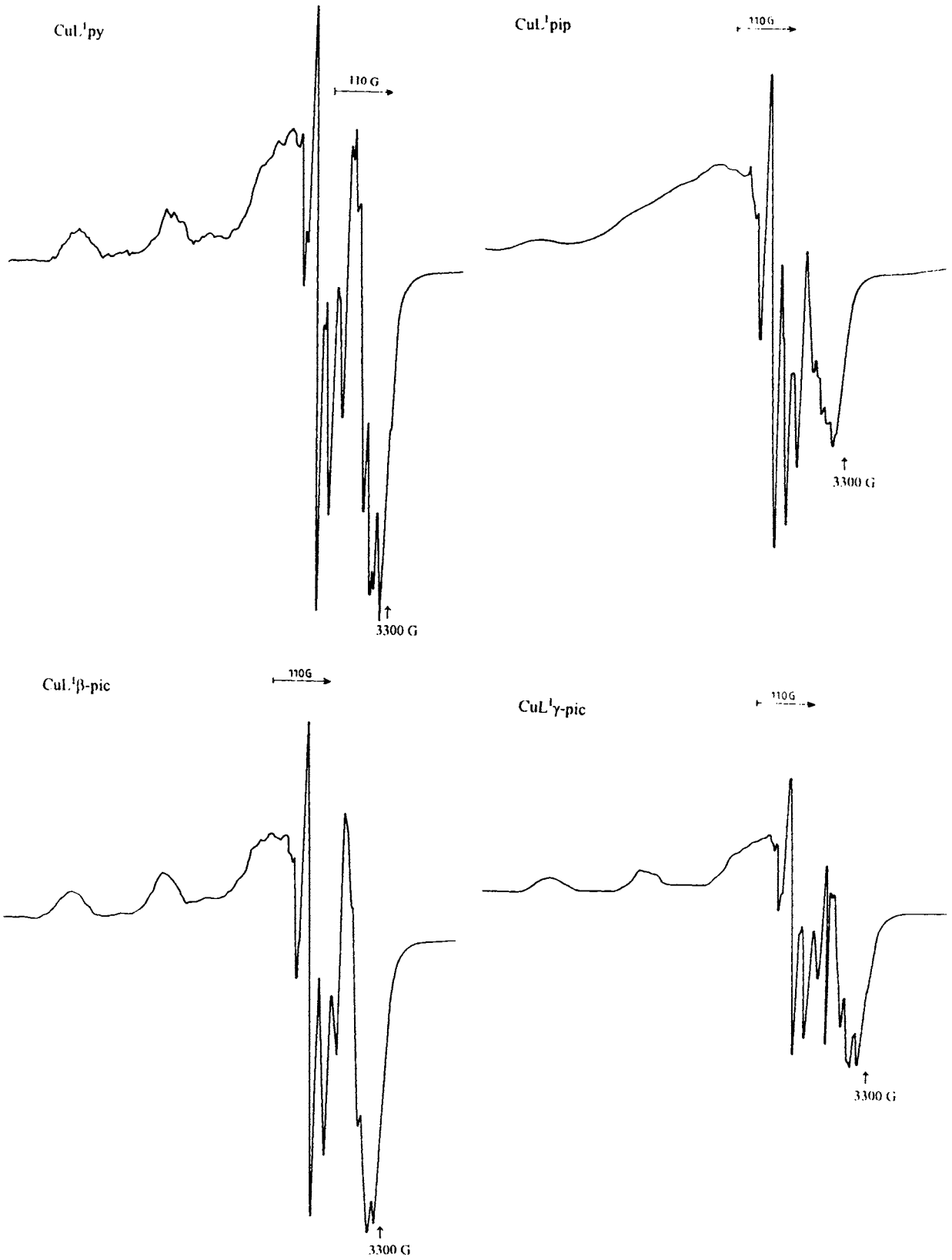

Figure 3.3 EPR spectra of Cu(II) complexes in DMF at 113 K

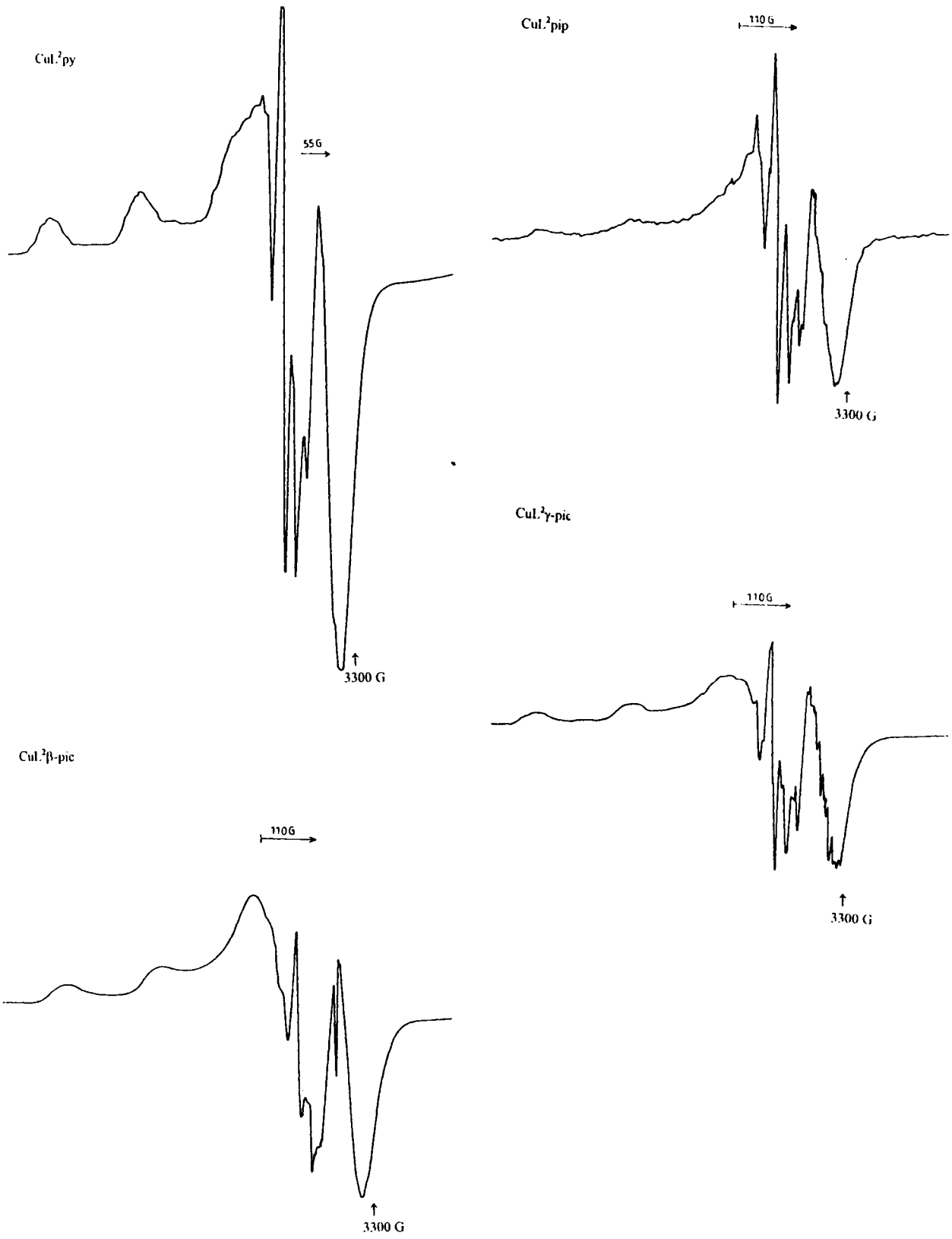

Figure 3.3 EPR spectra of Cu(II) complexes in DMF at 113 K

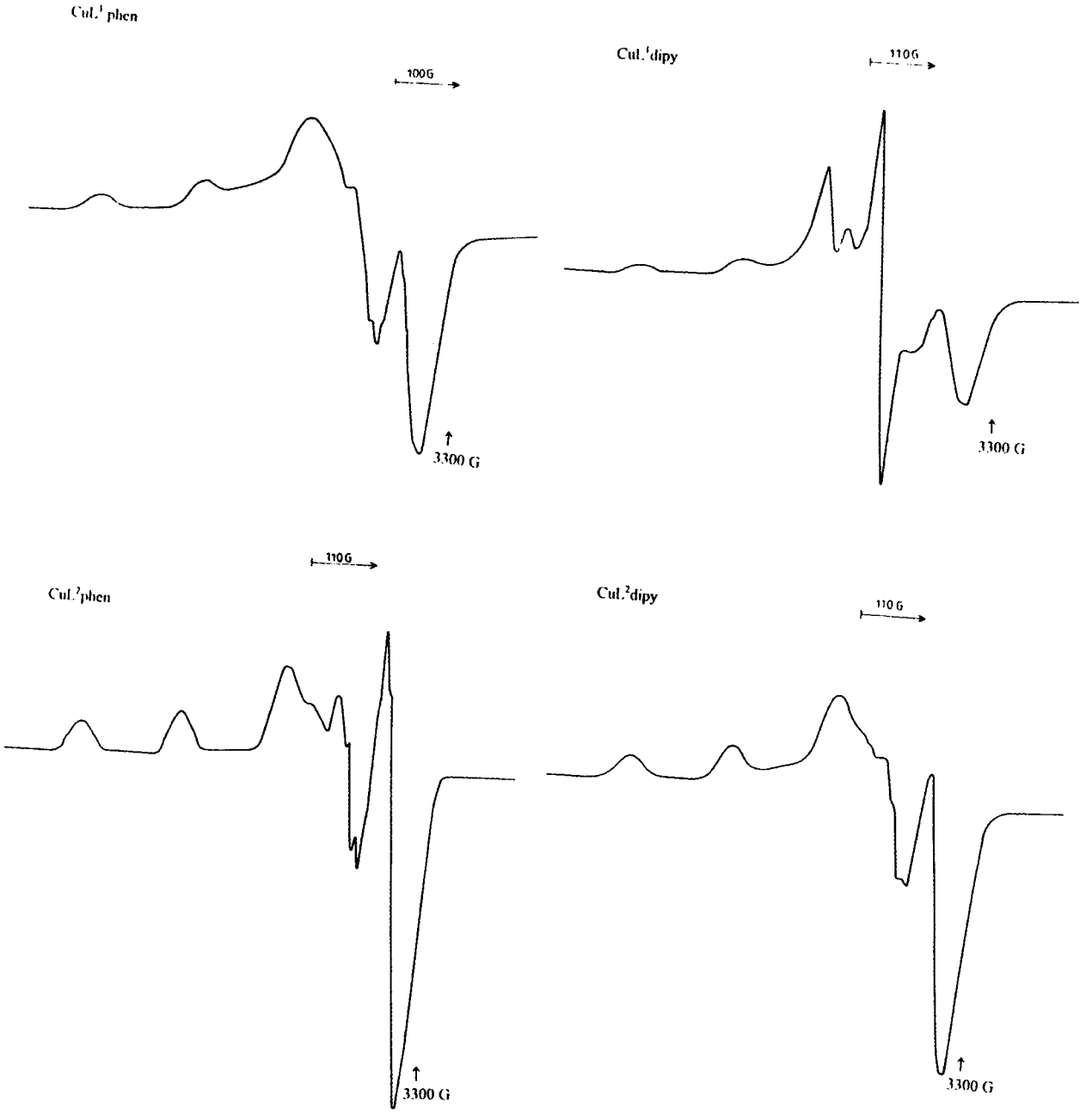

Figure 3.4 EPR spectra of Cu(II) complexes in DMF at 113 K

Table 3.7 Spin Hamiltonian and bonding parameters of copper(II) salicylaldehyde ^4N-phenylthiosemicarbazone complexes

	CuL^1py	CuL^1pip	$CuL^1\beta$-pic	$CuL^1\gamma$-pic	CuL^1phen	CuL^1dipy
Polycrystalline (300 K)						
$g_{\parallel}$	----	----	2.146	2.143	2.135	----
$g_{\perp}$	----	----	2.042	2.059	2.078	----
g_{av} or g_{iso}	2.056	2.097	2.073	2.076	2.087	2.097
DMF (77 K)						
$g_{\parallel}$	2.181	2.185	2.182	2.184	2.189	2.183
$g_{\perp}$	2.049	2.054	2.047	2.048	2.061	2.086
g_{av}	2.094	2.097	2.092	2.093	2.103	2.118
$A_{\parallel}$ (Cu) $\times 10^{-4}$	196.40	193.09	196.88	195.79	191.81	189.57
$A_{\perp}$ (Cu) $\times 10^{-4}$	36.73	41.19	38.33	40.19	42.11	67.47
$A_{av} \times 10^{-4}$	89.96	91.82	91.18	92.06	92.00	108.17
G	3.64	3.44	3.84	3.89	3.11	2.14
α^2	0.78	0.78	0.79	0.78	0.78	0.78
β^2	0.60	0.62	0.61	0.60	0.64	0.62
γ^2	0.64	0.70	0.64	0.64	0.80	0.73
K	0.34	0.35	0.34	0.34	0.35	0.41
$K_{\parallel}$	0.68	0.69	0.69	0.69	0.70	0.69
$K_{\perp}$	0.71	0.74	0.71	0.71	0.79	0.76

Table 3.8 Spin Hamiltonian and bonding parameters of copper(II) salicylaldehyde ^4N-cyclohexylthiosemicarbazone complexes

	CuL^2py	CuL^2pip	$CuL^2\beta$-pic	$CuL^2\gamma$-pic	CuL^2phen	CuL^2dipy
Polycrystalline (300 K) g_{iso}	2.085	2.056	2.078	2.089	2.096	2.074
DMF (113 K)						
$g_{\parallel}$	2.188	2.186	2.183	2.184	2.189	2.189
$g_{\perp}$	2.053	2.050	2.052	2.045	2.070	2.064
g_{av}	2.098	2.096	2.096	2.091	2.109	2.106
$A_{\parallel}$ (Cu) $\times 10^{-4}$	192.40	195.89	196.06	195.72	191.49	187.76
$A_{\perp}$ (Cu) $\times 10^{-4}$	35.04	36.75	43.66	38.39	56.54	46.68
A_{av} $\times 10^{-4}$	87.49	89.79	94.46	90.84	101.52	93.71
G	3.58	3.69	3.53	3.68	2.70	2.95
α^2	0.78	0.79	0.79	0.78	0.79	0.77
β^2	0.63	0.62	0.61	0.61	0.89	0.64
γ^2	0.67	0.65	0.67	0.64	0.91	0.66
K	0.34	0.34	0.36	0.34	0.38	0.36
$K_{\parallel}$	0.70	0.70	0.69	0.69	0.70	0.70
$K_{\perp}$	0.73	0.72	0.73	0.71	0.85	0.81

(Figure 3.4). The fact that $g_{\parallel}$ is greater than $g_{\perp}$ suggests a distorted square pyramidal structure and rules out the possibility of a trigonal bipyramidal structure which would be expected to have $g_{\perp} > g_{\parallel}$ Thus the coordination polyhedron comprises one phenanthroline/dipyridyl nitrogen, the azomethine nitrogen, the thiolate sulfur, the phenolate oxygen of the thiosemicarbazone (which form the base of the pyramid) and the remaining phenanthroline/dipyridyl nitrogen (which occupies the axial position) as shown below.

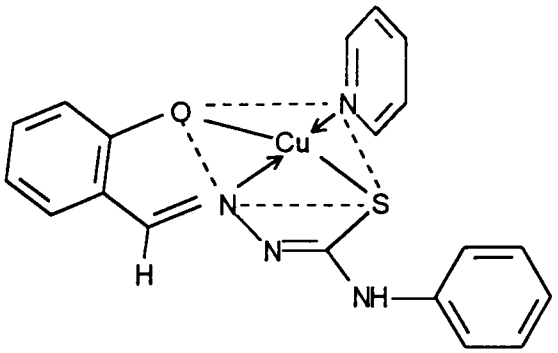

a) $CuL^{1}py$

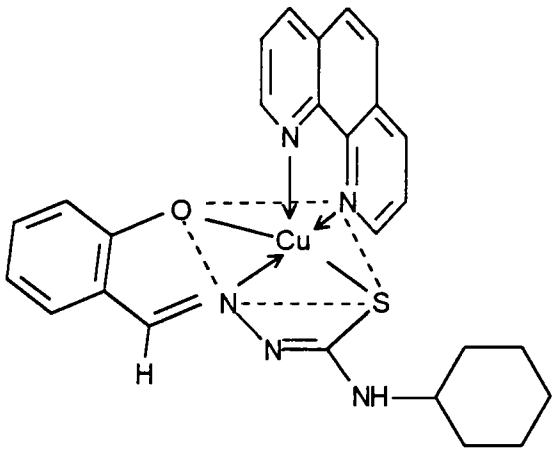

b) $CuL^{2}phen$

Figure 3.5

The EPR parameters $g_{\parallel}$, $g_{\perp}$, g_{av}, $A_{\parallel}$(Cu) and $A_{\perp}$(Cu) and the energies of d–d transition were used to evaluate the bonding parameters α^2, β^2 and γ^2, which may be regarded as measures of the covalency of the in-plane σ bonds, in-plane π bonds, and out-of-plane π bonds respectively.

The $g_{\parallel}$ values are nearly the same for all the complexes indicating that the bonding is dominated by the thiosemicarbazone moiety rather than the heterocyclic bases. The fact that the $g_{\parallel}$ values are less than 2.3, is an indication of significant covalent bonding in these complexes [75, 76].

In all the complexes $g_{\parallel} > g_{\perp} > 2.00$ and $G = (g_{\parallel} - 2)/(g_{\perp} - 2)$ values are < 4.4, are in consistent with a $d_{x^2-y^2}$ ground state having a small exchange coupling [77],

The value of in-plane sigma bonding parameter α^2 was estimated from the expression [75],

$$\alpha^2 = A/0.036 + (g_{\parallel} -- 2.0023) + 3/7\,(g_{\perp} -- 2.0023) + 0.04$$

The following simplified expressions were used to calculate the bonding parameters [78],

$$g_{\parallel} = 2.00 + (8K_{\parallel}^2 \lambda_0) / [E(d_{x^2-y^2} - d_{xy})]$$

$$g_{\perp} = 2.00 + (2K_{\perp}^2 \lambda_0) / [E(d_{x^2-y^2} - d_{xz}\, d_{yz})]$$

where $K_{\parallel} = \alpha^2\beta^2$, and $K_{\perp} = \alpha^2\gamma^2$, $K_{\parallel}$ and $K_{\perp}$ are orbital reduction factors and λ_0 represents the one electron spin orbit coupling constant which equals -828 cm^{-1}.

Hathaway [79] has pointed out that, for pure σ bonding, $K_{\parallel} \approx K_{\perp} \approx 0.77$, and for in-plane π bonding, $K_{\parallel} < K_{\perp}$; while for out-of-plane π bonding, $K_{\perp} < K_{\parallel}$. In all the

complexes it is observed that $K_{\parallel} < K_{\perp}$ which indicates the presence of significant in-plane π bonding. Furthermore α^2, β^2 and γ^2 have values much less than 1.0, which is expected for 100% ionic character of the bonds, and become smaller with increasing covalent bonding. Therefore, the evaluated values of α^2, β^2 and γ^2 of the complexes are consistent with both strong in-plane σ and in-plane π bonding.

The Fermi contact hyperfine interaction term K may be obtained from expression [80],

$$K = A_{iso} / P\beta^2 + (g_{av} - 2.0023) / \beta^2$$

where P is the free ion dipolar term and its value is 0.036. K is a dimentionless quantity, which is a measure of the contribution of s electrons to the hyperfine interaction and is generally found to have a value of 0.30. The K values obtained for all the complexes are in good agreement with those estimated by Assour [81]; Abragam and Pryce [82].

3.3.5 Cyclic voltammetry

The electrochemical properties of metal complexes particularly with sulfur donor atoms have been studied in order to monitor spectral and structural changes accompanying electron transfer [83]. Cyclic voltammetric measurements were carried out in the case of pyridine, 1,10-phenanthroline and dipyridyl copper(II) complexes. Measurements were made on the degased (N_2 bubbling for 15 min.) solutions in DMF (10^{-3} M) containing 0.1 M tetrabutylammonium perchlorate (TBAP) as the supporting electrolyte. The three electrode system consisted of glassy carbon (working), platinum wire (counter) and Ag/AgCl (reference) electrodes.

The number of electrons (n) involved in the reaction has been experimentally found to be one. Examination of the experimental data shows that the reduction

of copper(II) is quasireversible except for CuL^1phen, which is irreversible. In this type of electron transfer process, the current is controlled by a mixture of diffusion and charge transfer kinetics and can be identified by the following criteria [84], ΔE_p (= E_a - E_c) is greater than 59 mV and increases with increasing V. I_a/I_c is equal to unity only for $\alpha = 0.5$ (α is the charge transfer-coefficient).

The quasireversibility associated with the reduction based on the the E° value, probably arises from the relaxation process involved in a stereochemical change from copper(II) to copper(I) [85]. The copper(II) to copper(I) redox processes are influenced by the coordination number, stereochemistry and the hard/soft character of the ligands' donor atoms. However due to inherent difficulties in relating coordination number and stereochemistry of the species present in solution, redox processes are generally described in terms of the nature of the ligands present [86]. Patterson and Holm [87] have shown that softer ligands tend to produce more positive E° values, while hard acids give rise to negative E° values. The observed E° values for the five thiosemicarbazone complexes indicate considerable "hard acid" character which is likely to be due to azomethine nitrogen donor and nitrogen atom(s) of the heterocyclic bases involved in coordination. The results of our cyclic voltammetric studies of the Cu(II) complexes are summarised in Tables 3.9 and 3.10 and representative cyclic voltammograms (C.V.) for the behaviour of CuL^1dipy and CuL^2py are shown in the Figure 3.6.

The results of this spectral, magnetic and EPR study of the Cu(II) complexes suggest that the thiosemicarbazones act as tridentate O-N-S ligands, and the fourth (and fifth) coordination site is occupied by the nitrogen atom(s) of the heterocyclic base. The legends provide a substantially covalent environment with important in-plane σ and π bonding contributions.

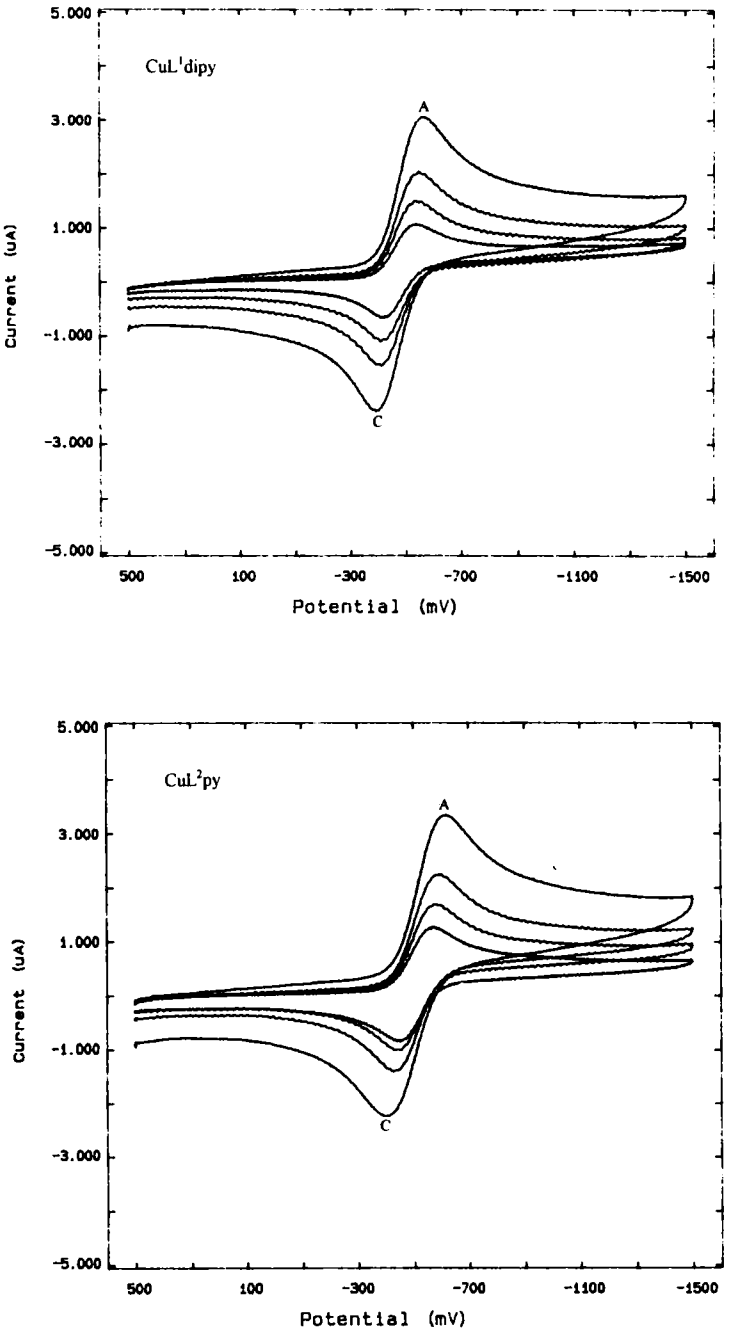

Figure 3.6 Cyclic voltammogram (scan rate 50-500 mV s^{-1}) for 10^{-3} M CuL^1dipy and CuL^2py at 300 K

Table 3.9 Cyclic voltammetric data for the copper(II) complexes of salicylaldehyde ^4N-phenylthiosemicarbazone

Scan rate (mVs^{-1})	E_p(A) (Vs^{-1})	E_p(C) (Vs^{-1})	E° (Vs^{-1})	ΔE_p (Vs^{-1})	i_{pa}/i_{pc}
			$CuL^1py{\cdot}3H_2O$		
50	0.55	0.45	0.50	0.10	1.06
100	0.56	0.43	0.49	0.13	1.10
200	0.57	0.42	0.49	0.15	1.11
500	0.59	0.40	0.50	0.19	1.04
			CuL^1dipy		
50	0.52	0.43	0.47	0.09	1.00
100	0.53	0.41	0.47	0.12	1.00
200	0.54	0.41	0.47	0.13	1.00
500	0.56	0.39	0.47	0.17	1.05
			$CuL^1phen{\cdot}H_2O$		
50	1.01	0.46	0.73	0.55	1.50
100	1.02	0.43	0.72	0.59	2.00
200	1.02	0.41	0.72	0.61	1.90
500	1.05	0.38	0.72	0.67	2.00

Table 3.10 Cyclic voltammetric data for copper(II) complexes of salicylaldehyde ^{4}N-cyclohexylthiosemicarbazone complexes

Scan rate ($mV\ s^{-1}$)	E_p (A) ($V\ s^{-1}$)	E_p (C) ($V\ s^{-1}$)	E° ($V\ s^{-1}$)	ΔE_p ($V\ s^{-1}$)	i_{pa}/i_{pc}
		$CuL^2py{\cdot}3H_2O$			
50	0.57	0.46	- 0.52	0.11	1.00
100	0.57	0.45	- 0.51	0.12	1.10
200	0.58	0.43	- 0.51	0.15	1.12
500	0.62	0.40	- 0.51	0.22	1.18
		$CuL^2dipy{\cdot}2H_2O$			
50	0.57	0.45	- 0.51	0.12	1.00
100	0.58	0.44	- 0.51	0.14	1.00
200	0.58	0.43	- 0.51	0.15	1.00
500	0.61	0.41	- 0.51	0.20	1.14

3.3.6 Biological activities

Biological activity in terms of their inhibitory property on specific known bacterial and fungal cultures were performed as follows.

Cultures

Bacterial and fungal cultures used for the present study were obtained from the Environmental Microbiology Laboratory of School of Environmental studies, Cochin University of Science and Technology. The bacterial cultures were maintained in nutrient agar slants and fungi in Sabouraud Dextrose Agar slants of the following composition.

Nutrient Agar

Peptone	: 0.5g
Buf extract	: 0.5g
Agar	: 2.0g
Distilled water	: 100 mL
pH	: 7.5 ± 0.2

Sabouraud Dextrose Agar

Peptone	: 1g
Dextrose	: 2g
Agar	: 2g
Distilled water	: 100 mL
pH	: 7 ± 0.2

Antibacterial and antifungal properties

Antibacterial and antifungal property of Salicylaldehyde ^4N-phenylthiosemicarbazone and its copper(II) complexes were determined by the standard 'disc diffusion' method. Here the bacteria and fungi were grown in nutrient and sabouraud dextrose agar slants and harvested the viable bacterial cells and fungal spore into phosphate buffered saline and swabbed on to nutrient agar and sabouraud dextrose agar plates respectively. The compounds to be tested were dissolved in DMF to a final concentration of 0.1% and soaked in filter paper discs of 5 mm diameter and 1 mm thickness. These filter papers were found to hold a quantity 0.01 mL solution. These discs were placed on the already seeded plates and incubated at 28 ± 0.4° C for 48 to 72 h. A clearing zone around the disc indicated the inhibitory activity of the compound on the organism.

The results of antibacterial and antifungal studies were given in Table 3.11. Out of twelve cultures tested, CuL^1phen exhibits wide spectrum of activity, it is active against nine cultures and next is CuL^1dipy, active against eight cultures. In general the ^4N-phenylthiosemicarbazone is found to be less active than its base adducts of Cu(II) complexes. Salicylaldehyde ^4N-phenylthiosemicarbazone is found to be more active against bacteria and fungi than ^4N-cyclohexylthiosemicarbazone (section 4.3.5 Table 4.9) and indicate the presence of aromatic ring at ^4N position increases the activity. In the case of Cu(II) complexes it appears that, increase in coordination number from four to five increases microbial activity, this may be due to increase of lipid solubility as has been reported earlier [88].

Table 3.11 Antibacterial and antifungal studies of salicylaldehyde ^4N-phenylthiosemicarbazone and copper(II) complexes *(inhibition zone in cm)

	H_2L^1	CuL^1py	CuL^1pip	$CuL^1\beta$-pic	$CuL^1\gamma$-pic	CuL^1phen	CuL^1dipy
Bacterial Culture							
Shigella dysenteriae	—	—	—	—	—	+(0.9)	—
N.C.Staphy lococcus	—	—	+(1.8)*	+(1.4)	+(1.7)	+(1.0)	+(2.0)
Salmonella typhi	—	—	—	—	—	—	—
Photobacte rium sp.	—	+(0.8)	+(2.1)	—	+(0.9)	+(1.5)	+(1.6)
Staphylococcus aureus	+(1.7)	+(1.2)	+(1.4)	+(1.3)	+(1.4)	+(1.2)	+(1.3)
Fungal Culture							
Rhizoctonia	+(3.5-4.0)	+(2.3)	+(2.0-2.5)	+(2.0-2.5)	+(2.0-2.5)	+(2.0-2.5)	+(2.0-2.5)
Collectotrichium	—	+(0.9)	—	—	—	—	—
Aspergillus sp.(336)	+(5.0)	—	+(0.9)	+(0.9)	+(0.8)	+(0.9)	+(2.5)
Aspergillus sp.(340)	+(0.9)	+(0.5)	+(0.9)	+(0.9)	—	+(2.0)	+(0.9)
Aspergillus sp.(433)	+(0.7)	+(1.0)	+(0.7)	+(0.7)	+(0.7)	+(0.7)	+(0.7)
Aspergillus sp.(282)	—	—	—	—	—	+(0.7)	+(0.7)
Aspergillus sp.(333)	—	—	—	—	—	—	—
Total number of cultures sensitive	5	6	7	6	6	9	8

CAHPTER IV

SPECTRAL AND BIOLOGICAL STUDIES OF NICKEL(II) COMPLEXES

4.1 INTRODUCTION

Nickel(II) complexes are widely investigated by various physico-chemical techniques such as magnetic susceptibility measurements, ^{1}H and ^{13}C NMR, electronic and mass spectra. Usually Ni(II) complexes exhibit six coordinate octahedral, four coordinate tetrahedral or square planar geometries. Five coordinate geometry is rather unusual in Ni(II) complexes and when encountered exists as a result of particular circumstances in the complex rather than of any intrinsic tendency on the part of Ni(II) ion to attain the structure. Nickel(II) complexes derived from the thiosemicarbazones of aromatic *ortho*-hydroxy aldehydes, in particular salicylaldehyde have recently attracted considerable attention as homogeneous catalysts [89,90]. This chapter describes the synthesis, spectral characterization and biological activity of four- and five-coordinate mixed ligand complexes of Ni(II) with salicylaldehyde ^{4}N-monosubstituted thiosemicarbazones and heterocyclic bases.

4.2 EXPERIMENTAL

4.2.1 Materials

Details regarding the preparation and characterization of the ligands are given in Chapter II.

4.2.2 Synthesis of complexes

The mixed ligand complexes, NiL^1B and NiL^2B (where L^1 and L^2 are the dianion of salicylaldehyde ^4N-phenyl- and ^4N-cyclohexyl-thiosemicarbazones respectively, B = py, pip, β/γ-pic, imz, phen, or dipy) were prepared by mixing 2 mmol of the appropriate heterocyclic base in ethanol to a hot solution of thiosemicarbazone (2 mmol) in ethanol (20 mL). To this was added a hot solution of $Ni(OAc)_2 \cdot 4H_2O$ (0.498 g, 2 mmol) in ethanol (25 mL) with constant stirring. The mixture was heated under reflux for 8-12 h and the volume is reduced to half. The complexes separated overnight as microcrystalline powders, were thoroughly washed with hot water, hot ethanol, then ether and dried over P_4O_{10} *in vacuo*. Yield ~ 65%.

Binuclear Ni(II) complex of H_2L^2, $(NiL^2)_2$ was prepared by mixing $Ni(OAc)_2 \cdot 4H_2O$ (0.498 g, 2 mmol) in ethanol to a hot solution of cyclohexylthiosemicarbazone (0.544 g, 2 mmol) in ethanol, heated under reflux for 8 h. and the volume is reduced to half. The complex separated was collected, thoroughly washed with hot water, hot ethanol, then ether and dried over P_4O_{10} *in vacuo*. Yield ~ 70%.

4.2.3 Analytical methods

Details regarding the analytical methods and other characterization techniques are given in Chapter II.

4.3 RESULTS AND DISCUSSION

The colours, elemental analyses and stoichiometries of H_2L^1, H_2L^2 and its complexes are presented in Tables 4.1 and 4.2 respectively. These reveal the presence of one nickel atom, one molecule of dianionic thiosemicarbazone and one

Table 4.1 Colours, elemental analyses and magnetic moments of nickel(II) complexes of salicylaldehyde ^4N-phenylthiosemicarbazone

Compound	Colour	Found (Calcd.)% C	H	N	Ni	μ at 300 K (BM)
H_2L^1	Light yellow	61.87 (61.97)	4.70 (4.82)	15.35 (15.49)	—	—
NiL^1py	Brown	56.13 (56.05)	3.92 (3.96)	13.69 (13.76)	14.08 (14.39)	Diamagnetic
$NiL^1pip{\cdot}2H_2O$	Brown	50.89 (50.80)	5.67 (5.83)	12.34 (12.47)	12.95 (13.07)	Diamagnetic
$NiL^1\beta\text{-pic}{\cdot}H_2O$	Brown	54.59 (54.70)	4.38 (4.59)	12.87 (12.76)	13.66 (13.36)	1.44
$NiL^1\gamma\text{-pic}$	Brown	57.10 (57.04)	4.17 (4.30)	13.41 (13.30)	13.78 (13.94)	1.51
NiL^1imz	Red brown	51.75 (51.55)	3.67 (3.81)	17.65 (17.68)	14.90 (14.82)	3.53
$NiL^1dipy{\cdot}H_2O$	Dark brown	57.31 (57.39)	4.38 (4.21)	13.93 (13.94)	11.49 (11.69)	3.12
NiL^1phen	Dark brown	61.52 (61.44)	3.87 (3.76)	13.76 (13.78)	11.70 (11.55)	3.07

Table 4.2 Colour, analytical data, and magnetic moments of nickel(II) complexes of salicylaldehyde ^4N-cyclohexylthiosemicarbazone

Compound	Colour	Found (Calcd.)% C	H	N	Ni	μ at 300 K (B.M)
H_2L^2	Light yellow	60.14 (60.62)	6.73 (6.95)	15.31 (15.15)	—	—
$NiL^2py{\cdot}2H_2O$	Brown	50.01 (50.80)	5.74 (5.83)	12.06 (12.47)	13.08 (13.06)	Diamagnetic
$NiL^2pip{\cdot}3H_2O$	Brown	48.43 (48.22)	7.20 (7.24)	11.37 (11.83)	12.65 (12.40)	Diamagnetic
$NiL^2\beta pic{\cdot}2H_2O$	Brown	50.94 (51.80)	6.38 (6.09)	12.35 (12.09)	12.16 (12.66)	1.40
$NiL^2\gamma\text{-}pic{\cdot}2H_2O$	Brown	50.68 (51.80)	6.48 (6.09)	11.87 (12.09)	12.78 (12.66)	1.55
$NiL^2imz{\cdot}H_2O$	Red brown	49.04 (48.59)	5.21 (5.51)	16.02 (16.66)	14.09 (13.97)	3.56
$NiL^2dipy{\cdot}H_2O$	Dark brown	56.82 (56.71)	5.38 (5.35)	13.92 (13.74)	11.49 (11.55)	2.35
$NiL^2phen{\cdot}2H_2O$	Dark brown	56.80 (56.75)	5.45 (5.31)	13.03 (12.75)	10.70 (10.66)	2.24
$(NiL^2)_2{\cdot}H_2O$	Brown	47.81 (47.76)	4.44 (4.58)	11.62 (11.93)	16.90 (16.67)	Diamagnetic

heterocyclic base. The complexes are soluble in DMF and conductivity measurements (10^{-3} M solution in DMF) indicate that all complexes are non-conductors [51].

4.3.1 Magnetic susceptibilities

The room temperature magnetic susceptibility (corrected for diamagnetism) of all the complexes in the polycrystalline state are presented in Tables 4.1 and 4.2. The py, pip and $(NiL^2)_2$ are diamagnetic. The magnetic moments of β/γ -pic complexes are very low. Such low magnetic moments are known. The anomalous moments could be due to an equilibrium in the solid state between the square planar and tetrahedral structures [91], or could be due to a partial population of a spin triplet state [92] close to the idealised ground state $^1A_{1g}$ for D_{4h} symmetry. Penta-coordinate high spin complexes have magnetic moments in the 3.20 – 3.40 B.M. range [93]. The observed values of μ for phen and dipy complexes are slightly lower than those calculated for a high-spin penta coordinate trigonal bipyramidal configuration [94]. Low magnetic moment values have already been reported for Ni(II) complexes [95], which is thought to arise from quenching of the orbital contribution to the magnetic moment due to distortion of D_{3h} symmetry or due to strong in-plane π-bonding and axial ligation [96] as has been found in the case of some other Ni(II) complexes [97]. However in the absence of variable temperature magnetic measurements a detailed discussion is not feasible.

4.3.2 Vibrational spectra

The significant IR bands of H_2L^1, H_2L^2 and its Ni(II) complexes are presented in Tables 4.3 and 4.4 respectively along with their tentative assignments.

On coordination of azomethine nitrogen, $\nu(^7C=^1N)$ shifts to lower wave numbers by 15 - 25 cm^{-1}. The occurrence of ν(NN) at higher wavenumber in

Table 4.3 IR band assignments (cm^{-1}) for salicylaldehyde ^4N-phenylthiosemicarbazone and its nickel(II) complexes

Compound	ν(CN)	ν(CO)	ν(CS)	ν(NiN)	ν(NiO)	ν(NiS)	$\nu(NiN_{HB})$	Bands due to heterocyclic bases
H_2L^1	1622s	1259s	1333s, 792m	---	---	---	---	---
NiL^1py	1603s	1207s	1315s, 754m	398s	353m	297m	253s	1250s, 603w, 445s
$NiL^1pip{\cdot}2H_2O$	1605s	1213s	1320m, 754m	389sh	319m	297s	250s	1150m, 680w
$NiL^1\beta\text{-pic}{\cdot}H_2O$	1601s	1207m	1315s, 748m	360m	347s	297s	254m	1253s, 620w, 445s
$NiL^1\gamma\text{-pic}$	1601s	1205m	1313s, 748m	401s	354sh	278s	249s	1250s, 806s, 445s
NiL^1imz	1599s	1211s	1317s, 746m	414m	357s	295m	240s	2936m, 1371s, 1028m, 918m
$NiL^1dipy{\cdot}H_2O$	1599s	1180s	1311s, 742m	412s	393s	286m	249s	1250s, 1151m, 688s, 420w
NiL^1phen	1599s	1200s	1311s, 731s	409s	395s	294s	240s	1246s, 1145s, 684s, 410w

Table 4.4 IR band assignments (cm^{-1}) for salicylaldehyde ^4N-cyclohexylthiosemicarbazone and its nickel(II) complexes

Compound	ν(CN)	ν(CO)	ν(CS)	ν(NiN)	ν(NiO)	ν(NiS)	$\nu(NiN_{HB})$	Bands due to heterocyclic bases
H_2L^2	1620s	1269s	1334s, 860m	—	—	—	—	—
$NiL^2py{\cdot}2H_2O$	1602s	1209s	1316s, 850m	408s	362m	347s	248m	1266w, 596s, 450w
$NiL^2pip{\cdot}3H_2O$	1603s	1209s	1266m, 850w	408m	395m	360s	261m	1149s, 630s
$NiL^2\beta\text{-pic}{\cdot}2H_2O$	1603s	1210s	1267w, 833w	389m	362s	347s	251s	1253s, 613sh
$NiL^2\gamma\text{-pic}{\cdot}2H_2O$	1603s	1210s	1266w, 837m	390m	363s	347s	249s	1250m, 630s
$NiL^2imz{\cdot}H_2O$	1602s	1209s	1270m, 837s	390m	362s	347s	249s	1346w, 1030m, 922s
$NiL^2dipy{\cdot}H_2O$	1601s	1200s	1250m, 850m	394s	363s	317s	257s	1140w, 666sh, 420m
$NiL^2phen{\cdot}2H_2O$	1601s	1198m	1300m, 841s	396s	363s	333s	261m	1253s, 1149s, 680m, 410m
$(NiL^2)_2{\cdot}H_2O$	1602s	1209s	1260s, 846m	415s	365m	330s	----	----

the spectra of complexes compared to that of thiosemicarbazones confirm the coordination of azomethine nitrogen [22]. A band at 385 - 415 cm^{-1} is assigned to ν(NiN) for these complexes. On loss of -^{2}NH proton, coordination *via* the thiolate sulfur [98] is indicated by a decrease in the frequency (20 - 80 cm^{-1}) of the ν(C=S) bands found at 1333 and 792 cm^{-1} for H_2L^1 and for H_2L^2 these bands were found at 1334 and 860 cm^1. The presence of a new band at 275 - 360 cm^{-1} assignable to ν(NiS) is another indication of the involvement of sulfur coordination. The phenolic oxygen on loss of -OH proton, occupies the third coordination site, causing ν(CO) to shift to lower wavenumbers by 50 - 80 cm^{-1} in the complexes. A new band at 320 - 395 cm^{-1} is assignable to ν(NiO) for these complexes. The coordination of heterocyclic N atom(s) is confirmed by the presence of ν(NiN) at 240 - 260 cm^{-1} range. A band around 3600 cm^{-1} indicate the presence of lattice water in these complexes [99].

The spectrum of $(NiL^2)_2$ exhibits a medium intensity band at 740 cm^{-1} may be attributable to the Ni$<^{O}_{O}>$Ni ring vibration [45, 100].

4.3.3 Electronic spectra

The significant electronic absorption bands in the spectra of the complexes recorded in DMF and Nujol mull are presented in Tables 4.5 and 4.6.

The electronic spectra of thiosemicarbazones were explained in section 3.3.3 (Chapter III). The electronic spectra of all the complexes are dominated by two bands or shoulders at 37,000 - 42,000 cm^{-1} range ($\pi \rightarrow \pi^*$) and at 26,000 - 34,900 cm^{-1} range ($n \rightarrow \pi^*$), which can be assigned to aromatic ring and thiosemicarbazone moiety respectively. NiLpy, NiLpip (L = L^1 or L^2) and $(NiL^2)_2$ exhibit a shoulder at 16,660- 17,740 cm^{-1} ($^1A_{1g} \rightarrow {}^1A_{2g}$) and a high intensity broad band at 23,400 - 23,870 cm^{-1} ($^1A_{1g} \rightarrow {}^1B_g$). The high intensity of the latter band may be due to overlap of L → M charge transfer band. The high

Table 4.5 Electronic spectra (cm^{-1}) (log ε in parentheses)[a] of salicylaldehyde ^4N-phenylthiosemicarbazone and its nickel(II) complexes

Compound	State	d–d	L → M	n → π*	π → π*
H_2L^1	DMF	—	—	28,570sh(4.05) 32,380(3.92)	39,060(3.47)
	Mull	—	—	27,660 32,480	40,620
NiL^1py	DMF	16,880sh(2.00)	23,860(4.08), 26,670(4.31)	31,700sh(4.24)	39,390(4.03)
	Mull	16,990sh	23,470, 26,460	29,070	41,490
$NiL^1pip{\cdot}2H_2O$	DMF	16,670sh(2.22)	23,750(4.09), 26,670(4.31)	31,700sh(4.26)	39,390(4.15)
	Mull	16,920sh	23,420, 26,600	29,070	41,940sh
$NiL^1\beta$-pic$\cdot H_2O$	DMF	17,000sh(2.06)	23,810(4.07), 26,670(4.29)	31,710sh(4.22)	39,390(4.15)
	Mull	11,900sh 17,460sh	23,920, 26,740	28,890	42,550
$NiL^1\gamma$-pic	DMF	17,220sh(2.07)	23,810(4.12), 26,670(4.34)	31,700sh	39,220(4.18)
	Mull	11,640sh 17,440sh	23,370, 25,840	29,240	41,320
NiL^1imz	DMF	17,240sh(2.12)	23,700(4.06), 26,600(4.25)	31,330sh(4.20)	39,210(4.18)
	Mull	11,580sh 17,600sh	23,640, 25,490sh	28,890	41,500
$NiL^1dipy{\cdot}H_2O$	DMF	17,000sh(2.12)	24,100(4.00), 26,600(4.46)	28,890(4.33)	40,000sh(3.90)
	Mull	17,540sh	23,750sh, 27,080sh	29,070	41,270sh
NiL^1phen	DMF	17,330sh(2.12)	24,040(4.17), 26,670(4.29)	31,700sh(4.27)	39,390(4.27)
	Mull	17,650sh	23,420sh, 26,600	29,070	41,840

[a] ε are given in units of $dm^3\ mol^{-1}\ cm^{-1}$

Table 4.6 Electronic spectral assignments (cm^{-1}) (log ε in parentheses)[a] for the salicylaldehyde ^4N-cyclohexylthiosemicarbazone and its nickel(II) complexes

Compound	State	d--d	L → M	n → π*	π→π*
H_2L^2	DMF	---	---	25,525sh(4.00) 32,100sh(3.93)	39,215sh(3.57)
	Nujol	---	---	28,260sh, 31,325sh	41,270sh
$NiL^2py{\cdot}2H_2O$	DMF	16,665sh(2.18)	24,215sh(4.00)	26,805sh(4.26), 32,500sh(4.11)	37,145(4.30), 40,625sh(4.38)
	Nujol	17,390sh	23,420sh 24,270sh	27,960sh, 32,100sh	39,370
$NiL^2pip{\cdot}3H_2O$	DMF	16,665sh(2.24)	24,215sh(4.07)	26,530(4.28), 32,910sh(4.21)	36,765(4.38), 40,000sh(4.31)
	Nujol	17,740sh	23,245sh 23,925sh	27,700, 31,705sh	39,680
$NiL^2\beta\text{-}pic{\cdot}2H_2O$	DMF	17,450sh(2.24)	24,155sh(3.99)	26,530sh(4.19), 32,300sh(4.11)	36,765(4.29), 41,270sh(4.26)
	Nujol	11,710sh 17,890sh	26,635sh 24,275	27,625, 31,710sh	40,820
$NiL^2\gamma\text{-}pic{\cdot}2H_2O$	DMF	17,005sh(2.24)	24,155(4.06)	26,525(4.25), 32,500(4.22)	36,630(4.34), 42,015(4.29)
	Nujol	12,000sh 17,190sh	23,245sh 24,530sh	27,370sh, 30,950sh	38,760
$NiL^2imz{\cdot}H_2O$	DMF	16,720sh(2.56)	24,215(3.95)	26,530sh(4.16), 32,500sh(4.11)	36,495(4.23), 40,000sh(4.22)
	Nujol	11,580sh 17,600sh	23,245sh 23,925sh	27,370sh, 31,745sh	38,165
$NiL^2dipy{\cdot}H_2O$	DMF	17,095sh(2.12)	24,075sh(3.67)	27,365sh(4.02), 32,910sh(4.11)	35,715(4.36)
	Nujol	17,765sh	24,295sh 25,490sh	27,659sh, 31,325sh	39,525sh
$NiL^2phen{\cdot}2H_2O$	DMF	17,390sh(2.24)	24,390sh(3.89)	26,925sh(4.12), 30,230(4.32)	36,900(4.55), 40,385sh(4.36)
	Nujol	17,795sh	26,000sh	31,705sh	40,295
$(NiL^2)_2{\cdot}H_2O$	DMF	16,600sh	24,330(3.80)	27,100(4.20), 31,950sh(4.04)	39,060(4.93)

[a] ε are given in units of $dm^3\ mol^{-1}\ cm^{-1}$

intensity band or broad shoulder at 23,365 - 26,670 cm^{-1} correspond to L → M and is associated with $^1A_{1g} \rightarrow {}^1E_g$ transition. The absence of bands below 10,000 cm^{-1} confirms the planar nature of these complexes. This is because of the large crystal field splitting in a square planar complex, the energy separation between the $d_{x^2-y^2}$ orbital and the next lower orbital is invariably greater than 10,000 cm^{-1} [101].

In T_d symmetry Ni(II) give rise to a $^3T_1$(F) ground state. $^3T_1$(F) → $^3T_1$(P) state (ν_3) occurs in the visible region (15,150 cm^{-1}), but for low symmetry T_d complexes the band is observed at 20,000 -- 15,150 cm^{-1} and bands are also occur at 11,900 -- 10,000 cm^{-1} and 9000 cm^{-1} due to $^3T_1$(F) → $^3A_2$(F) transition (ν_2) [101]. The complexes prepared from imidazole, exhibit characteristic bands at 17,600 and 11,580 cm^{-1} due to ν_3 and ν_2 transitions respectively, which indicate T_d symmetry and magnetic moment values support this. No absorption due to ν_1 is observed.

β/γ-picoline complexes exhibit a highly intense broad band or shoulder which overlaps with L → M charge transfer band and observed at 23,360 - 24,000 cm^{-1}. These complexes exhibit bands due to tetrahedral complexes in addition to square planar complexes. This indicates the possible presence of tetrahedral ⇌ square planar equilibrium in these complexes.

The electronic spectra of Ni(II) complexes of phen and dipy do not resemble the spectra of other five-coordinate Ni(II) complexes [97, 102], but are similar to those of pseudo-octahedral Ni(II) complexes [44, 101].

4.3.4 NMR spectra

^{1}H and ^{13}C NMR spectra of the thiosemicarbazones were discussed in section 2.3 (Chapter II). ^{1}H and ^{13}C NMR spectra (300 MHz) of diamagnetic Ni(II) complexes recorded in $CDCl_3$ - DMSO-d_6 mixture are presented in Tables 4.7 and

4.8 respectively. -OH and -^{2}NH protons of thiosemicarbazones are absent in the ^{1}H NMR spectra of complexes, because of their loss on complexation. Absence of -^{2}NH proton signal suggests the enolisation of -^{2}NH--C=S group to -^{2}N=C–SH and subsequent coordination through deprotonated thiolate. Considerable shift of characteristic signals occur on complexation. A signal at 3.21 ppm with an integration corresponding to four protons in the spectrum of NiL^{1}pip may be attributed to two lattice water molecules. The NMR spectral datum of $(NiL^{2})_2$ shows the presence of two ligand moieties, indicating a dimeric structure with Ni$<^{O}_{O}>$Ni linkage.

The ^{13}C NMR data support the coordination of the thiosemicarbazones through the phenoxy oxygen, azomethine nitrogen and thiolate sulfur, because deshielding or shielding of carbon atoms occur on coordination.

The spectral data prove that the Ni(II) ternary complexes prepared from pyridine, piperidine and β/γ-picolines have square planar, for imidazole tetrahedral and for phenanthroline and dipyridyl complexes five coordinate pseudo-octahedral geometry, with the thiosemicarbazones acting as ONS tridendate ligand and N-atom(s) of heterocyclic base occupying the fourth (and fifth) coordination site about the Ni(II) atom. Square planar dimeric structure with Ni$<^{O}_{O}>$Ni linkage may be suggested for $(NiL^{2})_2$ complex.

Table.4.7 ^{1}H and ^{13}C NMR spectral data of salicylaldehyde ^{4}N-phenylthiosemicarbazone and its nickel(II) complexes (δ ppm)[a] in DMSO-d_6

Compound	^{1}H NMR			^{13}C NMR			
	--CH=N--	--^{4}NH	Aromatic	--C--O--	--CH=N--	>C=S	Aromatic
H_2L^1	8.37(1)	7.26(1)	6.84-7.60(9)	156.52	144.57	175.54	116.20, 118.33, 119.20, 124.72, 125.23 127.96, 129.27, 131.05,138.22
NiL^1py	8.82(1)	8.29(1)	6.60-7.76(14)	153.20	161.18	164.60	114.82, 118.24, 119.10, 121.18, 124.01 128.02, 131.40, 131.87,137.60,140.50, 151.51
$NiL^1pip{\cdot}2H_2O$	8.90(1)	7.83(1)	6.62-7.57(9)	152.72,	159.51	164.89	114.90, 118.25, 120.79, 122.00, 124.00, 127.69, 131.00, 131.38, 140.37

[a] Integration values are given in parentheses

Table 4.8 ^{1}H and ^{13}C NMR spectra of salicylaldehyde ^{4}N-cyclohexylthiosemicarbazone and its nickel(II) complexes (δ ppm)[a] in DMSO-d_6

Compound	^{1}H NMR				^{13}C NMR			
	-CH=N-	-^{4}NH	Aromatic	Aliphatic	-C-O-	-CH=N-	-C=S	Aromatic[b] & Aliphatic[c] carbons
H_2L^2	8.11(1)	6.59(1)	7.25-7.35(4)	1.18-2.17(11)	157.38	147.07	175.26	(120.33, 131.75, 117.25, 132.35, 116.85)[b] (53.41, 32.69, 24.72, 25.49)[c]
$NiL^2py{\cdot}2H_2O$	8.86(1)	6.64(1)	6.80-7.78(9)	1.16-2.01(11)	158.00	143.90	160.20	(113.65, 129.90, 116.59,130.44, 113.65, 130.44, 122.45, 142.37)[b] (52.96, 31.08, 22.61, 23.32)[c]
$NiL^2pip{\cdot}3H_2O$	8.14(1)	6.54(1)	6.68-7.60(4)	1.07-1.91(21)	157.94	143.55	160.50	(117.76, 128.80, 116.76, 129.90,114 00)[b] (24.80, 26.40, 45.89, 51.98, 31.48, 23.17, 23.70)[c]
$(NiL^2)_2{\cdot}H_2O$	8.07(2)	6.58(2)	7.41-7.60(8)	1.11-1.93(22)				

[a] Integration values are given in parentheses

4.9. ^{4}N-cyclohexylthiosemicarbazone and Ni(II) complexes do not exhibit any activity against *Salmonella typhi*, *Photobactericm sp.* and *Shigella dysenteriae*. Some Ni(II) complexes exhibit profound activity against *Aspergillus sp.* than their uncomplexed thiosemicarbazone i.e. metal complexes are more fungitoxic than the free ligands. This could be understood in terms of chelation theory [103], stating that upon complexation the polarity of the metal ion gets reduced which increases the lipophilicity of the metal complexes facilitating them to cross the cell membrane easily.

Table 4.9 Antibacterial and antifungal studies of salicylaldehyde ^4N-cyclohexylthiosemicarbazone and nickel(II) complexes *(inhibition zone in cm)

	H_2L^2	NiL^2py	NiL^2pip	$NiL^2\beta$-pic	$NiL^2\gamma$-pic	NiL^2imz	NiL^2phen	NiL^2dipy
Bacterial culture								
Salmonella typhi	—	—	—	—	—	—	—	—
Non-coagulace *Staphylococcus*	+(0.70)*	+(0.60)	+(0.90)	—	—	—	+(0.60)	—
Photobacterium sp.	—	—	—	—	—	—	—	—
E. coli	—	—	—	+(0.50)	—	—	—	+(0.60)
Shigella dysenteriae	—	—	—	—	—	—	—	—
Fungal culture								
Rhizoctonia	+(0.60)	—	—	—	—	—	—	—
Colloectotrichium	—	—	—	—	—	—	—	—
Aspergillus sp.(282)	—	+(1.00)	—	+(0.70)	—	—	—	—
Aspergillus sp.(333)	—	—	—	—	+(0.70)	+(1.30)	+(0.60)	+(0.90)
Aspergillus sp.(336)	—	—	—	—	—	—	—	—
Aspergillus sp.(340)	—	—	—	—	—	—	—	—
Aspergillus sp.(433)	—	—	—	—	—	—	—	—

CHAPTER V

SPECTRAL CHARACTERIZATION OF COBALT(II) COMPLEXES

5.1 INTRODUCTION

Planar cobalt(II) complexes have received considerable attention in the past, mainly from two different angles. Cobalt(II) complexes of Schiff bases and related ligands have been considered as possible catalysts for the activation of molecular oxygen [104 - 109]. Cobalt(II) complexes of thiosemicarbazones were important because of their antitumour [110], antimicrobial [111], and electrical properties [111,112]. This chapter describes the isolation and characterization of cobalt(II) complexes of ^4N-monosubstituted salicylaldehyde thiosemicarbazones containing heterocyclic bases.

5.2 EXPERIMENTAL

5.2.1 Materials

Details regarding the preparation and characterization of the ligands are given in Chapter II.

5.2.2 Synthesis of complexes

The mixed ligand complexes, CoL^1B and CoL^2B (where L^1 and L^2 are the dianion of salicylaldehyde ^4N-phenyl and ^4N-cyclohexylthiosemicarbazones respectively. B is pyridine, piperidine, imidazole, 1,10-phenanthroline or 2,2'-dipyridyl) were prepared by mixing 2 mmol of the appropriate heterocyclic base in ethanol with a hot solution of thiosemicarbazone (2 mmol) in ethanol (30 mL). To

this was added a hot and filtered solution of $Co(OAc)_2 \cdot H_2O$ (0.498 g, 2 mmol) in ethanol (25 mL) with constant stirring. The mixture was heated under reflux for 8--10 h. and the volume is reduced to half. The complexes separated as microcrystalline powders were thoroughly washed with hot water, hot ethanol, then ether and dried over P_4O_{10} *in vacuo*. Yield ~ 70%.

5.2.3 Analytical methods

Details regarding the analytical methods and other characterization techniques are given in Chapter II.

5.3 RESULTS AND DISCUSSION

The colours, elemental analyses, stoichiometries of H_2L^1, H_2L^2 and its complexes are presented in Tables 5.1 and 5.2 respectively. This indicate 1:1:1 stoichiometry for Co-L-B (L = L^1 or L^2). The complexes are insoluble in most of the common polar and non-polar solvents. They are soluble in DMF and conductivity measurements (10^{-3} M solution in DMF) indicate that all complexes are non-conductors [51].

5.3.1 Magnetic susceptibilities

The room temperature magnetic susceptibility of the complexes, py, pip and imz in the polycrystalline state fall in the 2.50 – 2.62 B.M. range, which are expected for a low spin square planar Co(II) complex [93]. The magnetic moments of Co(II) complexes of phen and dipy are very low (2.80 – 2.92 B.M.) and lie in between high spin (4.70 – 5.10 B.M.) and low spin (2.00 – 2.50 B.M.) values showing the possibility of spin equilibrium to occur. Such low magnetic moment values for Co(II) complexes with S and N chelating agents were reported previously [113, 114]. The spin-equilibrium in penta-coordinate Co(II) complexes

Table 5.1 Colours, analytical data, magnetic moments, and EPR parameters of cobalt(II) complexes of salicylaldehyde ^4N-phenylthiosemicarbazone

Compound	Colour	Found (Calcd.)% C	H	N	Co	μ (B.M.) at 300 K	g_{iso} Polycrystalline 300 K	113 K
H_2L^1	Light yellow	61.87 (61.97)	4.70 (4.82)	15.35 (15.49)	-----	---	---	---
$CoL^1py{\cdot}H_2O$	Brown	53.54 (53.65)	4.33 (4.26)	13.00 (13.17)	13.21 (13.86)	2.69	2.075	2.079
$CoL^1pip{\cdot}H_2O$	Brown	52.52 (52.89)	5.00 (5.60)	12.73 (12.98)	13.71 (13.67)	2.50	2.074	2.061
CoL^1imz	Dark green	51.55 (51.52)	3.11 (3.81)	17.01 (17.66)	14.29 (14.88)	2.62	2.036	----
$CoL^1phen{\cdot}2H_2O$	Dark brown	57.83 (57.36)	4.09 (4.25)	13.00 (12.86)	10.55 (10.83)	2.88	2.668	2.276
$CoL^1dipy{\cdot}2H_2O$	Dark brown	55.28 (55.38)	4.25 (4.45)	13.24 (13.45)	11.51 (11.33)	2.43	2.338	----

Table 5.2 Colours, analytical data, magnetic moments, and EPR parameters of cobalt(II) complexes of salicylaldehyde ^4N-cyclohexylthiosemicarbazone

Compound	Colour	Found (Calcd.)% C	H	N	Co	μ (B.M.) at 300 K	g_{iso} Polycrystalline 300 K	113 K
H_2L^2	Pale yellow	60.14 (60.62)	6.73 (6.95)	15.31 (15.15)	----	----	----	---
$CoL^2py{\cdot}H_2O$	Brown	52.75 (52.89)	5.32 (5.60)	13.13 (12.99)	13.81 (13.67)	2.60	2.119	2.287
$CoL^2pip{\cdot}H_2O$	Brown	52.26 (52.16)	6.89 (6.91)	13.05 (12.81)	13.59 (13.48)	2.62	2.297	----
$CoL^2imz{\cdot}H_2O$	Dark green	48.19 (48.56)	5.12 (5.51)	16.41 (16.65)	13.85 (14.03)	2.59	2.136	----
$CoL^2phen{\cdot}3H_2O$	Dark brown	54.26 (54.92)	5.22 (5.49)	12.63 (12.31)	10.00 (10.37)	2.92	2.088	----
$CoL^2dipy{\cdot}3H_2O$	Dark brown	52.39 (52.93)	5.29 (5.73)	13.01 (12.86)	10.59 (10.83)	2.74	2.071	2.071

is governed [115] by the nature of donor groups and geometric distortion of the chromophore. Unfortunately, due to the nonaccessibility of variable temperature magnetic measurements facility, we are unable to determine the cross-over temperatures.

5.3.2 Vibrational spectra

The significant IR bands of H_2L^1, H_2L^2 and its Co(II) complexes are presented in Tables 5.3 and 5.4 respectively along with their tentative assignments. The IR spectrum of all the complexes indicate that the thiosemicarbazones coordinate *via* O, N and S as explained before. The coordination of N atom(s) of heterocyclic base is confirmed by the appearance of ν(CoN) in the 279 – 299 nm range. Appearance of new bands at 410 – 450, 370 – 409 and 300 – 358 cm^{-1} range corresponds to ν(CoN) [116], ν(CoO) [117] and ν(CoS) [116, 118] respectively.

5.3.3 Electronic spectra

The significant electronic absorption bands in the spectra of all the complexes, recorded in DMF and Nujol mull are persented in Tables 5.5 and 5.6.

Electronic spectra of thiosemicarbazones were explained in section 3.3.3 (Chapter III). In the electronic spectra of these Co(II) complexes, i.e. py, pip and imz the observed absorption bands are indicative of D_{2h} symmetry for the Co(II) d^7 planar stereochemistry [119]. A shoulder occuring at 14,5000 – 15,7000 cm^{-1} is assigned to the transitions $^2A_g \rightarrow {}^2B_{1g}$ ($d_{x^2-y^2} \rightarrow d_{xy}$) and $^2A_g \rightarrow {}^2B_{3g}$ ($d_{xz} \rightarrow d_{xy}$). Two shoulders around 22,000 cm^{-1} and another one at 25,000 cm^{-1} are assigned to the $^2A_g \rightarrow {}^2B_{2g}$ ($d_{xz} \rightarrow L(\pi^*)$) and $^2A_g \rightarrow {}^2B_{3g}$ ($d_{yz} \rightarrow L(\pi^*)$) metal-to-ligand charge transfer transitions respectively.

Table 5.3 IR band assignments (cm^{-1}) for the salicylaldehyde ^4N-phenylthiosemicarbazone and its cobalt(II) complexes

Compound	ν(CN)	ν(CO)	ν(CS)	ν(CoN)	ν(CoO)	ν(CoS)	ν(CoN_{HB})	Bands due to heterocyclic bases
H_2L^1	1622s	1259m	1333s, 792m	---	---	---	---	---
$CoL^1py{\cdot}1H_2O$	1599s	1197s	1300m, 750s	432s	379s	302s	288m	1240s, 603w, 465m
$CoL^1pip{\cdot}H_2O$	1599s	1198s	1292s, 750m	430s	388m	315s	290w	1150m, 640w
CoL^1imz	1597s	1197s	1300sh, 750s	438s	391m	330m	288w	1371s, 918m
$CoL^1phen{\cdot}2H_2O$	1595s	1194s	1311s, 723s	450m	400m	340m	297m	1467s, 750w,588m
$CoL^1dipy{\cdot}2H_2O$	1595s	1194m	1311s, 740s	441m	409m	358m	299m	1449vs, 1095s, 754m, 410w

Table 5.4 IR band assignments (cm^{-1}) for the salicylaldehyde ^4N-cyclohexylthiosemicarbazone and its cobalt(II) complexes

Compound	ν(CN)	ν(CO)	ν(CS)	ν(CoN)	ν(CoO)	ν(CoS)	$\nu(CoN_{HB})$	Bands due to heterocyclic bases
H_2L^2	1620s	1629s	1335s, 860s	—	—	—	—	—
$CoL^2py{\cdot}H_2O$	1601s	1199s	1292s, 822m	417s	370m	300s	280m	1245w, 455w
$CoL^2pip{\cdot}H_2O$	1599s	1200s	1300m, 821s	410s	377m	305s	284m	1152w, 630m
$CoL^2imz{\cdot}H_2O$	1601s	1199m	1290s, 848m	415s	378s	307s	279m	1346s, 1050m, 920w
$CoL^2phen{\cdot}3H_2O$	1597s	1197s	1266m, 846s	430s	399s	313s	290m	1470s, 730s, 515w
$CoL^2dipy{\cdot}3H_2O$	1601s	1197s	1315s, 833m	422s	392m	329s	293m	1445s, 1096s, 750w

Table 5.5 Electronic spectral assignments (cm^{-1}) (log ε in parentheses)[a] for the salicylaldehyde ^4N-phenylthiosemicarbazone and its cobalt(II) complexes

Compound	State	d--d	L → M	n → π*	π → π*
H_2L^1	DMF	---	---	28,570sh(4.05) 32,380(3.92)	39,060(3.47)
	Nujol	---	---	27,660 32,485	40,625
$CoL^1py{\cdot}H_2O$	DMF	15,115sh(1.80)	22,600sh(4.14), 23,865sh(4.14) 24,300sh(4.10)	29,580(4.25) 32,500(4.61)	37,595(5.04)
	Nujol	15,125sh	23,000sh, 24,300sh	27,780, 32710sh	39,065
$CoL^1pip{\cdot}H_2O$	DMF	15,757sh(1.24)	22,605sh(4.10), 23,865sh(4.08) 25,490sh(4.04)	29,570sh(4.20) 32,500sh(4.54)	37,590(4.96)
	Nujol	14,705sh	23,010sh, 24,300sh	27,770, 32,725sh	39,065
CoL^1imz	DMF	15,295sh(1.41)	23,00sh(4.25), 23,810sh(4.25)	29,580(4.40) 32,700(4.76)	37,175(5.09)
	Nujol	14,815sh	23,000sh, 24,295sh	27,850, 32700	39,060
$CoL^1phen{\cdot}2H_2O$	DMF	18,570sh(2.83) 17,567sh(2.63) 14,925sh(1.40) 14,055sh(1.08)	22,610sh(4.08), 24,040sh(4.08)	28,890(4.25) 32,500(4.57)	37,175(5.08)
	Nujol	14,800sh, 17920sh	22,220sh, 24,290sh	28,335, 31700	39,950
$CoL^1dipy{\cdot}2H_2O$	DMF	18,055sh(4.45) 16,775sh(2.80) 15,295sh(2.00) 14,605sh(1.80)	22,805sh(4.11), 23,870sh(4.12)	28,890(4.20) 32,100(4.59)	37,595(5.00)
	Nujol	16,665sh	22,605sh, 24,300sh	28,490sh, 32,100sh	39,840sh

[a]ε are given in units of $dm^3\ mol^{-1}\ cm^{-1}$

Table 5.6. Electronic spectral assignments (cm^{-1}) (log ε in parentheses)[a] for the salicylaldehyde ^4N-cyclohexylthiosemicarbazone and its cobalt(II) complexes

Compound	State	d--d	L → M	n → π*	π → π*
H_2L^2	DMF	---	---	25,525sh(4.00) 32,100sh(3.93)	39,215sh(3.57)
	Nujol	---	---	28,260sh, 31,325sh	41,270sh
$CoL^2py{\cdot}H_2O$	DMF	15,625sh(1.41)	23,215sh(3.97), 24,450(4.01)	26,805sh(3.97) 33,330sh(4.30)	37,875(4.75)
	Nujol	14,385sh	23,005sh, 24,300sh	28,770, 32,300	39,840
$CoL^2pip{\cdot}H_2O$	DMF	14,855sh(1.70)	23,215sh(4.03), 24,215(4.03)	27,660sh(4.02) 33,330sh(4.35)	37,880(4.70)
	Nujol	14,705sh	23,235sh, 24,365sh	28,490, 32,500sh	39,840
$CoL^2imz{\cdot}H_2O$	DMF	15,205sh(1.54)	23,425sh(3.66), 24,570sh(3.66)	28,260sh(3.67) 33,300sh(4.18)	37,175(4.23)
	Nujol	15,150sh	23,425sh, 24,530sh	28,700, 31,705	39,840
$CoL^2phen{\cdot}3H_2O$	DMF	17,575sh(2.58) 14,945sh(1.88) 14,285sh(2.50)	23,425sh(2.35), 24,450sh(2.35)	26,530sh(2.30) 34,210sh(4.40)	37,595(4.97)
	Nujol	15,575sh, 17,750sh	22,605sh, 24,300sh	28,490, 31705sh	39,840
$CoL^2dipy{\cdot}3H_2O$	DMF	15,660sh(2.75) 16,2500sh(2.39) 18,055sh(2.73)	23,425sh(4.03), 24,450sh(4.03)	26,260sh(4.17) 34,100sh(4.41)	37,590(4.66)
	Nujol	15,150sh, 16,665sh	22,605sh, 24,300sh	28,490, 32,100	39,840

[a] ε are given in units of $dm^3\ mol^{-1}\ cm^{-1}$

The electronic spectra of Co(II) complexes of phen and dipy resemble the spectra of other five-coordinate Co(II) complexes [101, 114], and a square pyramidal structure may be assigned for these complexes.

5.3.4 EPR spectra

EPR spectra of polycrystalline Co(II) complexes are recorded at 300 K and 110 K. Usually EPR spectra of Co(II) complexes do not give a well resolved spectra, but doping with isostructural diamagnetic host lattice will give a resolved spectra. Detailed study of EPR spectra in the present case has not been possible because of the failure to form a good glass with any of the solvents or solvent mixtures tried. The spectra of all the complexes show only one broad signal (Figure 5.1) which is attributable to the dipolar broadening and enhanced spin-lattice relaxation [62] of the coordinating ligand. The g values of all the complexes are given in Tables 5.1 and 5.2, indicate the presence of unpaired electron in d_{z^2} orbital [120, 121].

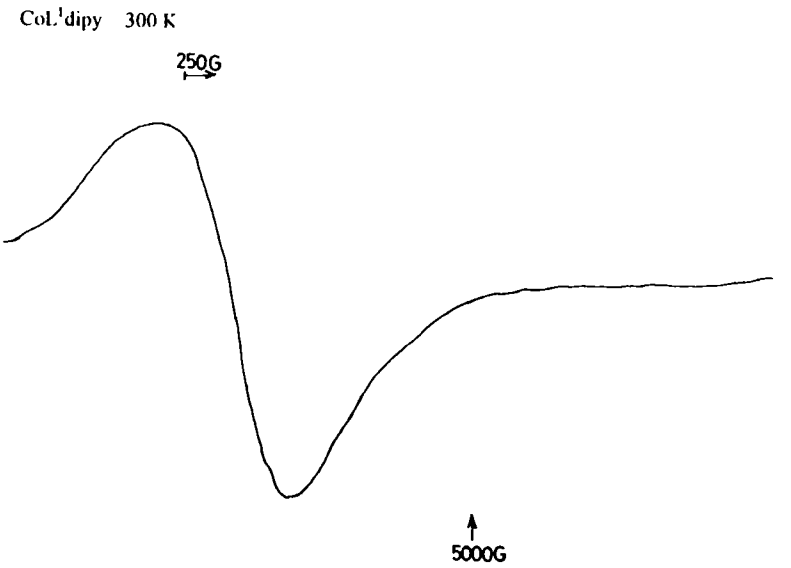

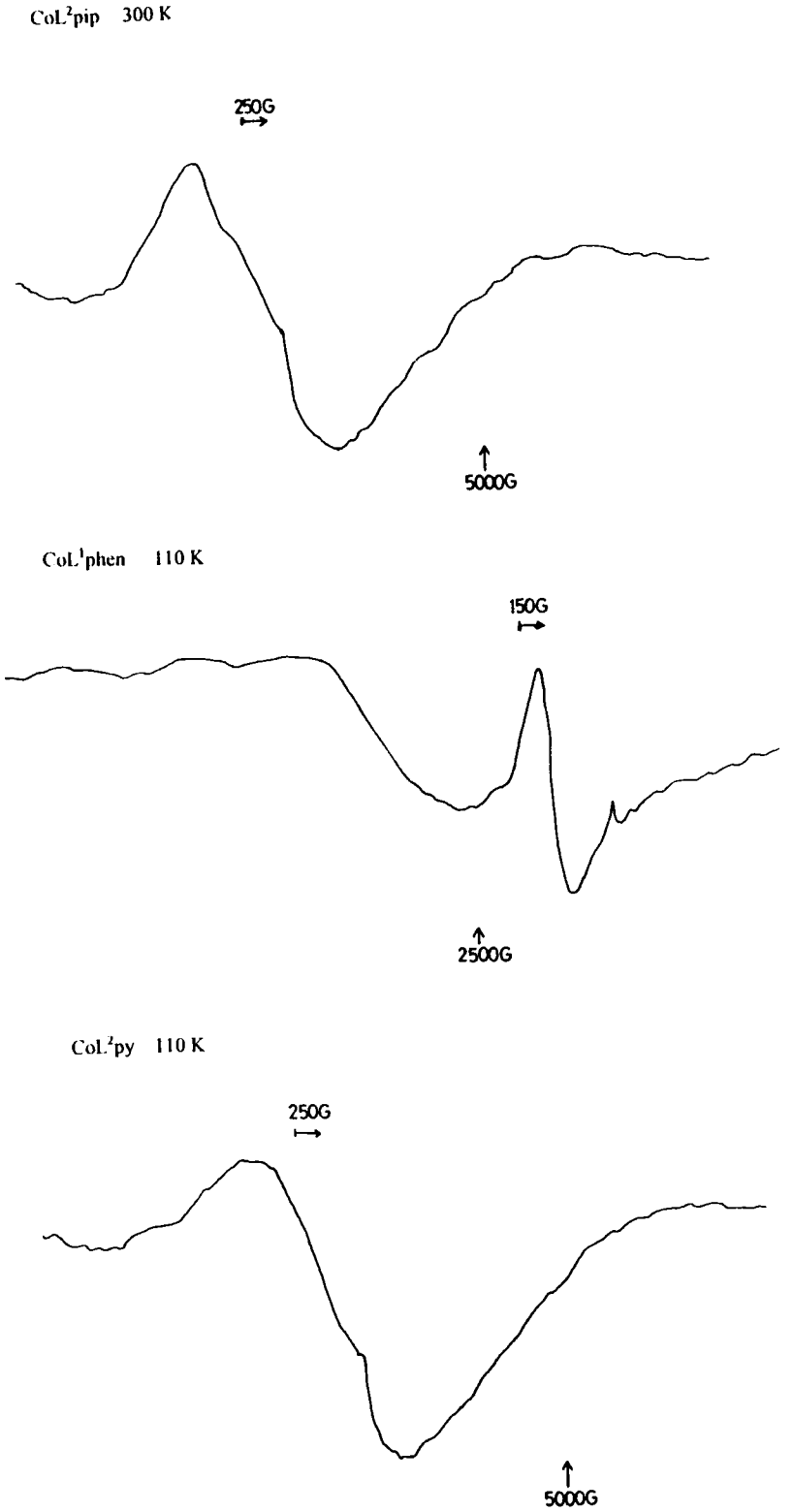

Figure 5.1 EPR spectra of Co(II) complexes in the polycrystalline state at 300 K and 110K

The spectral data indicate the presence of square planar geometry for py, pip, and imz complexes and a square pyramidal structure for phen and dipy complexes as shown in Figure 5.2.

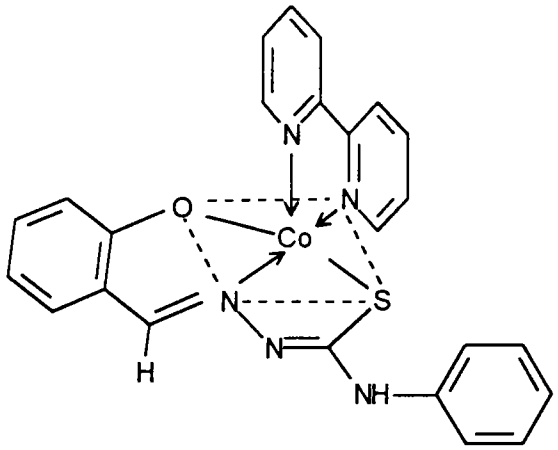

a) CoL^1dipy

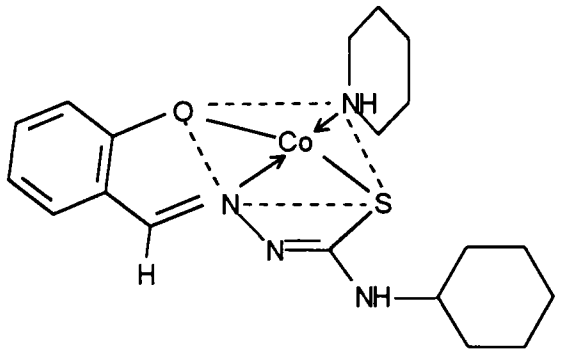

b) CoL^2pip

Figure 5.2

CHAPTER VI

SPECTRAL CHARACTERIZATION OF IRON(III) COMPLEX

6.1 INTRODUCTION

This chapter describes the isolation and characterization of iron(III) complex of salicylaldehyde ^4N-phenylthiosemicarbazone and piperidine. The complex has the composition FeL^1pipNO_3, (where L^1 = dianion of salicylaldehyde ^4N-phenylthiosemicarbazone). The complex has been characterized by elemental analysis, magnetic susceptibility measurement in the polycrystalline state at 300 K, IR, electronic, EPR spectra in the polycrystalline state at 300 K and 110 K and Mössbauer spectrum at 300 K.

6.2 EXPERIMENTAL

6.2.1 Materials

Details regarding the preparation and characterization of the ligand is given in Chapter II.

6.2.2 Synthesis of complex

The mixed ligand complex, FeL^1pipNO_3 was prepared by mixing 2 mmol of piperidine in ethanol to a hot solution of H_2L^1 (0.543 g, 2 mmol) in ethanol (20 mL). To this was added a hot and filtered solution of $Fe(NO_3)_3 \cdot 9H_2O$ (0.808 g, 2 mmol) in ethanol (40 mL) with constant stirring. The mixture was heated under reflux on a water bath for 16 h. The volume of the mixture was reduced to half. On cooling to ambient temperature, the complex which separated overnight as

microcrystalline powder, was thoroughly washed with hot water, hot ethanol, then ether and dried over P_4O_{10} *in vacuo*. Yield ~ 65%.

6.2.3 Analytical methods

Details regarding the analytical methods and other characterization techniques are given in Chapter II.

6.3 RESULTS AND DISCUSSION

Analytical data calculated for $C_{19}H_{22}N_5O_4SFe$: C, 48.32; H, 4.69; N, 14.82; Fe, 11.82; Found : C, 48.58; H, 4.79; N, 15.00; Fe, 11.70 reveals the presence of 1:1:1:1 stoichiometry for iron, thiosemicarbazone piperidine and genenion. The complex is soluble only in DMF and DMSO, and conductance value in DMF (10^{-3} M solution in DMF) indicates that it is a non-electrolyte [51].

6.3.1 Magnetic susceptibility

Iron(III) is known to exist in S = 5/2 (ground term $^6A_1$, μ = 5.92 B.M.), 3/2 (ground term $^4A_2$, μ = 4.00 B.M.) and 1/2 (ground term $^2T_2$, μ = 2.00 – 2.60 B.M.) states.

The magnetic susceptibility of the complex in the polycrysytalline state at 300 K is 4.55 B.M., which is in between S = 5/2 and S = 1/2. The obtained value is above the spin only value of 3.90 B.M. expected for five coordinate Fe(III) complexes with $^4A_2$ (S= 3/2) ground state. As the value is above 3.90 B.M., there may not be any possibility of antiferromagnetic exchange interaction.

6.3.2 Vibrational spectrum

The ν(OH) and ν(^{2}NH) bands of H_2L^1 disappears in the complex indicating the protonation of -OH and -^{2}NH protons. Coordination *via* the thiolate sulfur is indicated by a decrease in the frequency of the thioamide bands from 1333 and 792 cm^{-1} to 1317 and 752 cm^{-1} in the spectrum of complex [65]. A new band at 392 cm^{-1} corresponds to ν(FeS) confirms sulfur coordination. The ν(CO) band of H_2L^1 (1259 cm^{-1}) shifts to lower wavenumber (1200 cm^{-1}) in the spectrum of the complex and appearance of new band at 418 cm^{-1} due to ν(FeO) shows coordination *via* phenolate oxygen. The bonding of azomethine nitrogen to the metal ion is indicated by negative shift of ν(^{7}C=^{1}N) band from 1622 to 1602 cm^{-1}. Coordination of azomethine nitrogen is confirmed with the presence of a new band at 438 cm^{-1} assignable to ν(FeN) [8]. Absence of a band in the range 800 - 900 cm^{-1} rules out the possibility of Fe-O-Fe linkage in the complex [99]. Two medium intensity bands ν_1 and ν_4 observed at 1280 and 1383 cm^{-1} in the spectrum of complex suggest that nitrato group is monodentate [122]. A weak band at 362 cm^{-1} in the spectrum of the complex is assigned to ν(FeN) of piperidine. H_2L^1 coordinates *via* phenolate oxygen, azomethane nitrogen and thiolate sulfur and, fourth and fifth coordination sites are occupied by piperidine and nitrato group respectively.

6.3.3 Electronic spectrum

Electronic spectra of H_2L^1 and Fe(III) complex were recorded in DMF solution. The d-d bands are obscured as usual for Fe(III) complexes [123, 124]. The UV-region of the complex is dominated by $\pi \rightarrow \pi^*$ and two $n \rightarrow \pi^*$ transitions, corresponding to aromatic ring (38,235 cm^{-1}) and thiosemicarbazone moiety (28,890 and 32,910 cm^{-1}) respectively. A broad shoulder at 24,760 and 28,260 cm^{-1} may be due to $L \rightarrow M$ and $d \rightarrow \pi^*$ transitions respectively.

6.3.4 EPR spectrum

The EPR spectra of Fe(III) complex in the polycrystalline state at 300 and 110 K shows signals at $g \sim 4$ and $g \sim 2$, ($g_{\parallel} = 4.803$, $g_{\perp} = 2.016$ at 300 K and $g_{\parallel} = 4.709$, $g_{\perp} = 2.180$ at 110 K). Complete analysis of EPR spectra in the present case has not been possible because of the failure to form a good glass with any of the solvents or solvent mixtures tried. Figure 6.1 has definitely supported the five-coordinate stereochemistry for the complex as the appearance of signals at $g \sim 4$ and $g \sim 2$ could be explained by this geometry only. The EPR results for the systems with $^4A_2$ ground state can be described by the spin Hamiltonian [125 - 128],

$\mathcal{H} = D[\hat{S}_z^2 - 1/3\ S(S+1)] + E(\hat{S}_x^2 - \hat{S}_y^2) + g\beta HS$ with S = 3/2 and $g = 2.00$.

When E = 0 and also when D >> hν, there are two Kramers doublets $M_s = \pm 3/2$ and $\pm 1/2$, with effective g-tensor principal values $g_x = g_y = 0$; $g_z = 6$ and $g_x = g_y = g_z = 2$ as shown below.

D >> hν, E = 0

For the ($\pm 1/2$) doublet ignoring orbital contribution (since Fe(III) ion is $^6S_{5/2}$, L =0)

$$g_{xx} = g_{yy} = 2\left\langle +\frac{1}{2}\right| S_+ \left|-\frac{1}{2}\right\rangle$$

$$= 2\left\langle +\frac{1}{2}\right| (S_+ + S_-)2 \left|-\frac{1}{2}\right\rangle$$

$$= 2\sqrt{\left(\frac{3}{2}+\frac{5}{2}-\frac{1}{2}+\frac{1}{2}\right)}$$

$$= 2 = \sqrt{(4)} = 4$$

$g_{\perp} = 4$

$$g_{\parallel} = 2\left\langle \frac{1}{2} \middle| 2S_z \middle| \frac{1}{2} \right\rangle$$

$$= 2 \times 2 \times \frac{1}{2} = 2$$

For the $\pm\frac{3}{2}$ doublet

$$g_{\perp} = 2\left\langle +\frac{3}{2} \middle| 2S_{\perp} \middle| -\frac{3}{2} \right\rangle$$

$$= 2\left\langle +\frac{3}{2} \middle| S_+ + S_- \middle| -\frac{3}{2} \right\rangle$$

$$= 2 \times 0 = 0$$

$$g_{zz} = g_{\parallel} = 2\left\langle +\frac{3}{2} \middle| 2S_z \middle| +\frac{3}{2} \right\rangle$$

$$= 2 \times 2 \times \frac{3}{2} = 6$$

The complex under investigation show identical EPR properties (Figure 6.1) which may be described by the above Hamiltonian for E = 0. Such a system should give rise to g value of 6, 4 and 2. Here $g \sim 4$ is comparatively strong and becomes more sharp as temperature decreases and $g \sim 6$ signal is not observed since $|\pm 3/2|$ doublet is not expected to be populated appreciably [125].

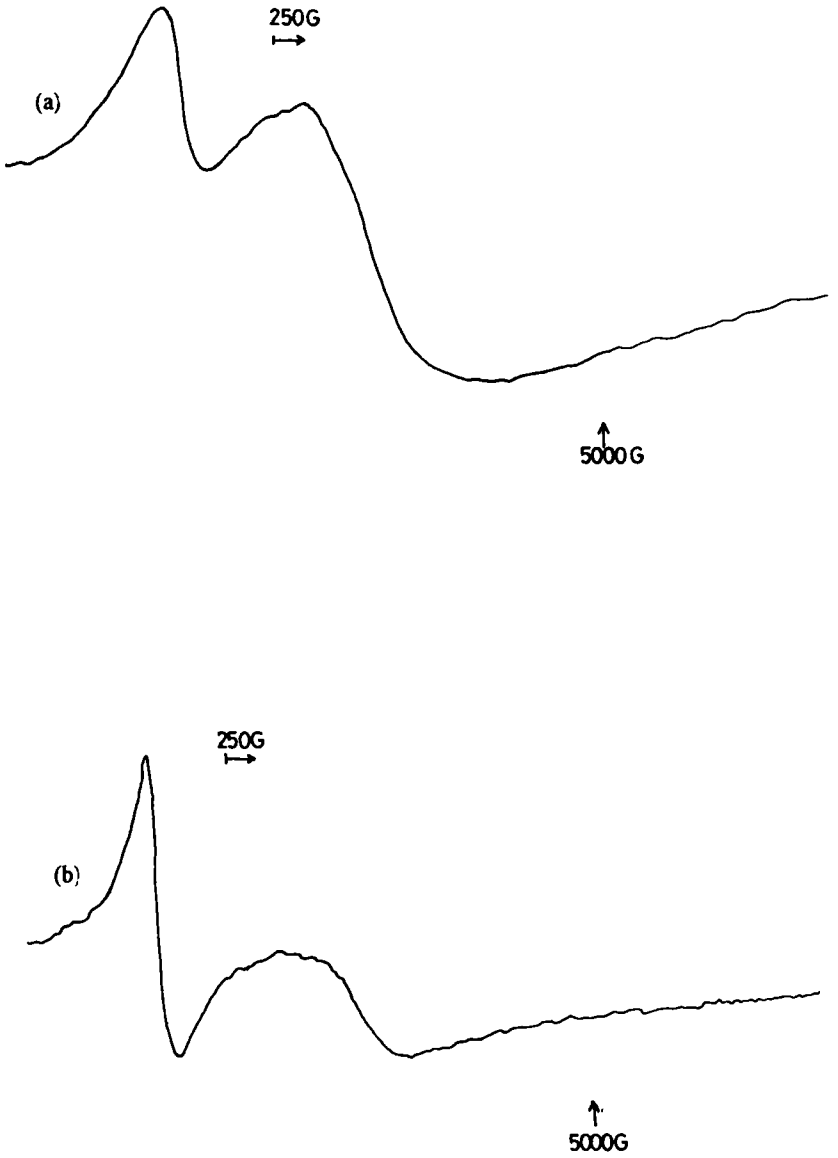

Figure 6.1 EPR spectra of iron(III) complex in the polycrystalline state at (a) 300 K (b) 110 K

6.3.5 Mössbauer spectrum

Mössbauer spectrum of the complex indicates the presence of two iron(III) species. The isomer shift (δ) and quadruple shift (ΔE_q) values are expected for a high spin Fe(III) complex.

The d^5 configuration of Fe(III), especially S = 3/2 exhibit isomer shift values in

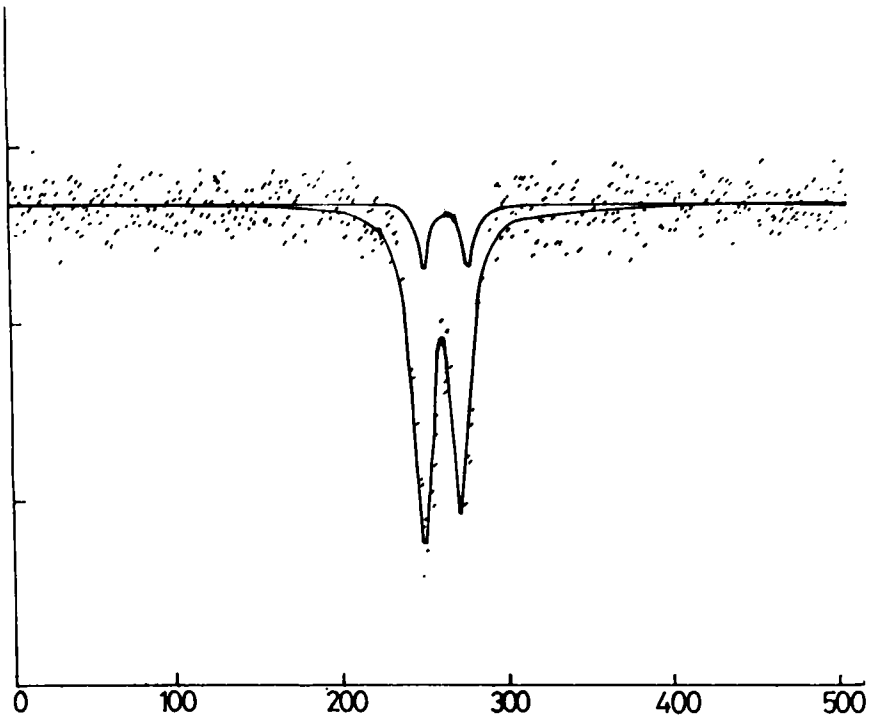

Figure 6.2 Mössbauer spectrum at 300 K

Table 6.1 IR, electronic, EPR and Mössbauer spectral data of Iron(III) complex of salicylaldehyde ^4N-phenylthiosemicarbazone

IR

ν(CN)	ν(CO)	ν(CS)	ν(FeN)	ν(FeO)	ν(FeS)	ν(FeN_{pip})	ν(ONO_2)
1602s	1200s	1317s	438m	418m	392w	362w	1280m
		752s					1383m

Electronic

d--d	L → M	n → π*	d → π*	π → π*
—	24,760sh(4.03)	28,890(4.41)	28,260sh(4.20)	38235(3.89)
		32,910sh(4.29)		

EPR

Polycrystalline state at

	300 K	110 K
$g_{\parallel}$	4.803	4.709
$g_{\perp}$	2.106	2.118

Mössbauer

Isomer shift (δ) (mm s^{-1})	Quadruple shift (ΔE_q) (mm s^{-1})	Line width (mm s^{-1})	Relative intensity
0.39	0.80	0.46	87.90
0.58	0.95	0.28	12.10

the range 0.2 – 0.5 mm s^{-1} [129]. Since the measured δ values are 0.39±0.05 mm s^{-1} has high s electron density hence the low δ value. The peak with large ΔE_q value (ΔE_q = 0.95±0.05 mm s^{-1}) suffers more asymmetric distribution around iron atom [129]. So it is assumed that highly intense peak corresponds to S = 3/2 and other S = 5/2.

Magnetic, EPR and Mössbauer studies reveal the existence of a quantum admixture of S = 3/2 and S = 5/2 states [130]. Quantum mechanical admixing presumed to be occur *via* spin-orbit coupling when the energy separation between the pure states is small, may be recognized also on the basis of unusual $g \approx 4$ ESR signals as well as by a drop in magnetic moment [131]. Based on these studies the following structure may be suggested for the complex.

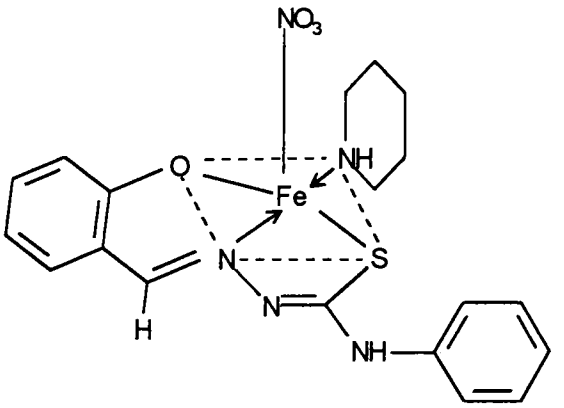

Figure 6.3 FeL^1pip

CHAPTER VII

CONDUCTOMETRIC STUDY OF MANGANESE(II) COMPLEXES OF THIOSEMICARBAZONES AS A FUNCTION OF TEMPERATURE

7.1 INTRODUCTION

Electrical conductivity measurement is well known for its wide range of applicability both in fundamental investigations of electrolyte solutions and in tackling many applied problems. Even though the measurement is very simple still it is more accurate method for those said investigations and analysis of substances in solution [132, 133]. Conductometric study is an important and versatile technique to establish the limiting molar conductance, theory of ion association and ion-solvent interaction.

In the present investigation manganese(II) complexes of acetone and butanone thiosemicarbazones are used as electrolytes for the study of ion-solvent interaction involved in the system in its aqueous solution from 283 - 313 K. Kraus-Bray equation is used for analysing conductance data and to establish limiting molar conductance and dissociation constant. Walden product and thermodynamic parameters of solvation process have been computed at all temperatures for the above two systems and reported. Limiting ionic conductance and ionic transport number of both the anion and cation of these complexes have been determined. All these values are used in the qualitative proposal of ion-solvent interaction involved in the system under the prevailing conditions.

The complexes under investigation namely *bis*(acetone thiosemicarbazone) manganese(II) sulfate and *bis*(butane thiosemicarbazone) manganese(II) sulfate were prepared as reported [134]. Eventhough M.H.

Hammamy *et al.* [52] studied electrical conductivity of some transition metal complexes of thiosemicarbazone, much attention has not been given to the study of thiosemicarbazone complexes. Hence the present study is undertaken.

7.2 EXPERIMENTAL

7.2.1 Materials

Details regarding the conductance measurements were given in Chapter II.

7.2.2 Synthesis of complexes

The Mn(II) complexes were prepared by mixing 1mmol of $MnSO_4$ and 2mmol of thiosemicarbazone in ethanol as reported previously [134]. The synthesised complexes were recrystallised in ethanol and dried over P_4O_{10} *in vacuo*. Known amount of complexes were separately dissolved in water and used in conductance measurements. Triply distilled water was used in the entire investigation.

7.3 RESULTS AND DISCUSSION

7.3.1 Molar conductance

The conductance offered by the solution of the two complexes, $Mn(ATSC)_2SO_4$ and $Mn(BTSC)_2SO_4$ was directly read from the instrument. The specific conductance and molar conductance were determined by usual methods. Kraus-Bray model [135] of conductivity was used for the evaluation of molar conductance at infinite dilution (limiting molar conductance

λ°_{m}) of the above two complexes at temperatures 283, 293, 303 and 313K in water. Kraus-Bray equation for 1:1 electrolyte used here can be represented as

$$\lambda_m C = \frac{1}{\lambda^{\circ}_m} + \frac{K_c \lambda^{\circ 2}_m C}{\lambda_m} \qquad (1)$$

where K_c is the dissociation constant

The plots of $\lambda_m C$ vs $1/\lambda_m$ were drawn and found to be linear (Figure 7.1). From the slope and intercept of these linear plots, limiting molar conductance and dissociation constant K_c were determined. Table 7.1 represents the limiting molar conductance (λ°_m) at different temperatures for the above two complexes. As can be seen molar conductance increases with decrease in complex concentration as expected. The resulted values of K_c at different temperatures for both the complexes are shown in Table 7.2. As expected limiting conductance increased with increase in temperature. Complex $Mn(BTSC)_2SO_4$ eventhough consists of relatively bulky butanone molecule compared to light acetone molecule of $Mn(ATSC)_2SO_4$. There is no much difference in λ°_m values and both the species have relatively equal mobility and transport numbers.

7.3.2 Effect of temperature

Increase in temperature increases the mobility of the conducting species of these two complexes. When the complexes are added to water, they dissolve, dissociate and destroy the three dimensional structure of water releasing more number of water molecules available for solvation. Both anion and cation of the complex get hydrated by water molecule. The hydration number of sulfate is found to be around 8 at lab temperature, which is exactly coinciding with the reported [136] value. It is known that hydration number slightly varies with

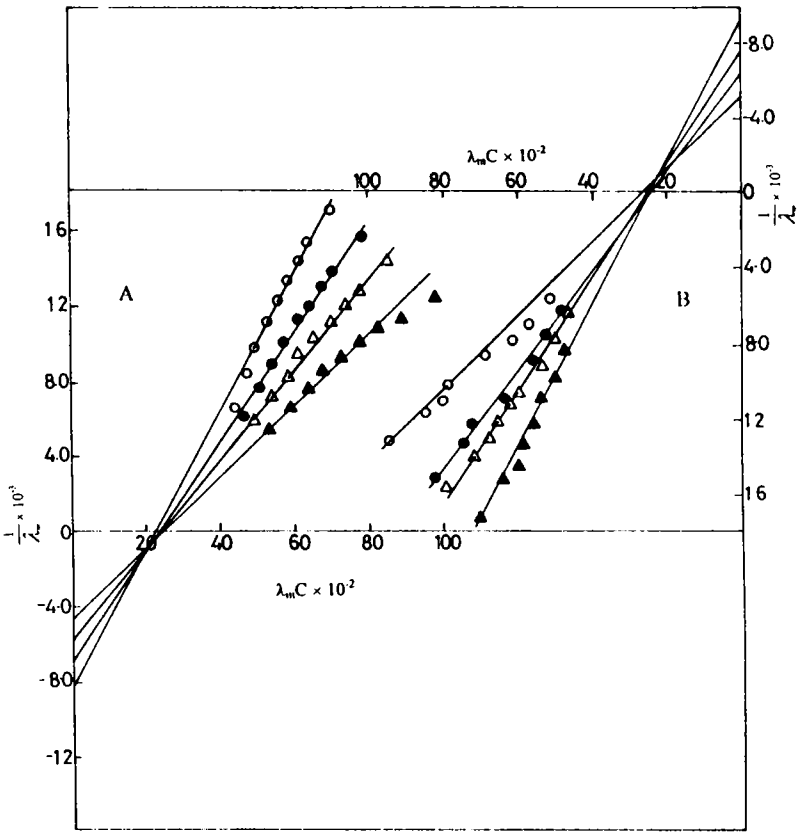

Figure 7.1 Plot of $\lambda_m C$ vs $\frac{1}{\lambda_m}$ for manganese(II) complexes at 283, 293, 303, 313 K

	283	293	303	313 K
A - $[Mn(ATSC)_2SO_4]$	o	•	Δ	▲
B - $[Mn(BTSC)_2SO_4]$	▲	Δ	•	o

Table 7.1 Estimated values of limiting molar conductances (λ^{o}_{m} ohm^{-1} cm^{2} mol^{-1}) for $Mn(ATSC)_2SO_4$ and $Mn(BTSC)_2SO_4$ at 283, 293, 303 and 313 K.

Complex	283 K	293 K	303 K	313 K
$Mn(ATSC)_2SO_4$	124	147	166	208
$Mn(BTSC)_2SO_4$	111	131	156	192

Table 7.2 Experimental dissociation constant K_c values for $Mn(ATSC)_2SO_4$ and $Mn(BTSC)_2SO_4$ at 283, 293, 303 and 313 K.

Complex	$K_c \times 10^{-2}$			
	283 K	293 K	303 K	313 K
$Mn(ATSC)_2SO_4$	3.74	2.92	2.32	1.94
$Mn(BTSC)_2SO_4$	3.84	3.08	2.73	1.94

temperature. In the present case hydration number of SO_4^{2-} is calculated at different temperatures for both the complexes using the following relations [137].

$$R = \frac{z F^2}{6\pi N_A \eta_o \lambda_m^\circ} = \frac{0.82|z|}{\eta_o \lambda_m^\circ} \qquad (2)$$

where R is the radius of a solvated ion and can also be calculated using the semi-empirical relationship based on the Stoke's law [138], which gives corrected radius R_s. The R_s values are presented in Table 7.3.

$$R_s = \frac{z F^2}{6\pi N_A \eta_o \lambda_m^\circ} + 0.013\varepsilon + r_y \qquad (3)$$

where R_s is the corrected radius of a solvated ion and γ_y = 0.1 A° for all anions [139], ε is the dielectric constant of the solvent.

$$\text{Solvation number} = \frac{R_s^3 - R_{cr}^3}{R_{(solvent)}^3} \qquad (4)$$

R_{cr} is the crystallographic radius obtained from literature [137]. Since crystallographic radius of the cationic moiety is not available, it was not possible to calculate the hydration number. As expected hydration number of sulfate ion decreases with increase in temperature and found to be 9, 8, 8 and 7 respectively at 283, 293, 303 and 313 K. That means the thermal energy has knocked off some water molecules from the primary hydration sheet of sulfate and these water molecules may conduct small amount of current at higher temperature. It is quite likely that some of water molecules may slightly dissociate and contributes its share towards conductance.

7.3.3 Dissociation constant

The ionisation constant (K_c) determined from Kraus-Bray plot is presented in Table 7.2. K_c decreased with increase in temperature in both the cases. According to Le-Chatelier's principle [140], increase in temperature brings about decrease in dissociation constant means, the system should act as exothermic in character i.e., change in enthalpy of dissociation ΔH_D should be negative. This is what has been experimentally found. The process may be represented as,

$$Mn(ATSC)_2SO_4 \rightleftharpoons [Mn(ATSC)_2]^{++} + SO_4^{2-} \quad \Delta H_D \text{ -ve.}$$

With the increase in temperature, the system favours the backward reaction. Therefore, more and more associated product will be obtained. That means association of species is increasing with increase in temperature which is observed experimentally. The K_c values of both these complexes decreases as the temperature is raised which is contrary to prediction from the electrostatic theories [139]. The change in enthalpy, entropy, and free energy of dissociation are estimated from the temperature dependence of the dissociation constant.

7.3.4 Activation parameters

Treating the conductance process equivalent to the rate process is well documented [141 - 143]. Therefore the following Arrhenius equation of rate process can be used to evaluate the activation energy related to the conductance process.

$$\lambda_m^\circ = A\, e^{-\frac{E_a}{RT}} \qquad (5)$$

$$\text{or } \log \lambda_m^\circ = \log A - \frac{E_a}{2.303RT} \qquad (6)$$

where A is a proportionality constant or frequency factor, E_a is the activation energy of the process which determine the rate of movement of ions. So the plot of log λ°_m vs 1/T (Figure 7.2) should be linear. From the slope and intercept of the linear plot, values of E_a and log A are determined and are found to be 12.4 kJ mol^{-1} and 4.4 for $Mn(ATSC)_2SO_4$ and 14.1 kJ mol^{-1} and 4.6 for $Mn(BTSC)_2SO_4$ respectively. Since the energy of the rate process and log A of the second complex are higher than that of the first complex, it is quite natural to have slightly lower limiting molar conductance for the second complex.

A plot of log K_c vs 1/T is drawn and found to be linear with a positive slope (Figure 7.3). From the slope of this plot change in enthalpy of the dissociation process (ΔH_D) (slope = $-\Delta H_D$ /2.303 R) are calculated and found to be −18.6 kJ mol^{-1} for $Mn(ATSC)_2SO_4$ and −20.4 kJ mol^{-1} for $Mn(BTSC)_2SO_4$. Both the values are negative, so the systems are exothermic as anticipated under effect of temperature on dissociation constant.

ΔG_D the change in free energy of dissociation and ΔS_D the change in entropy of dissociation are calculated using the following equations [138].

$$\Delta G_D = -2.303\ RT \log K_c \qquad (7)$$

$$\Delta S_D = \frac{\Delta H_D - \Delta G_D}{T} \qquad (8)$$

at different temperatures and resulted values are shown in Table 7.4. From the table it is clear that ΔG_D is positive for both the complexes, and slightly increasing with increase in temperature indicating the difficulty in dissociation of the complex with increase in temperature. In otherwords it may be stated that species are rather stable in gaseous phase than solution phase, because the positive value of ΔG_D indicates the non-spontaneity of the dissociation process. Hence it is very likely that association process is predominating with increase in

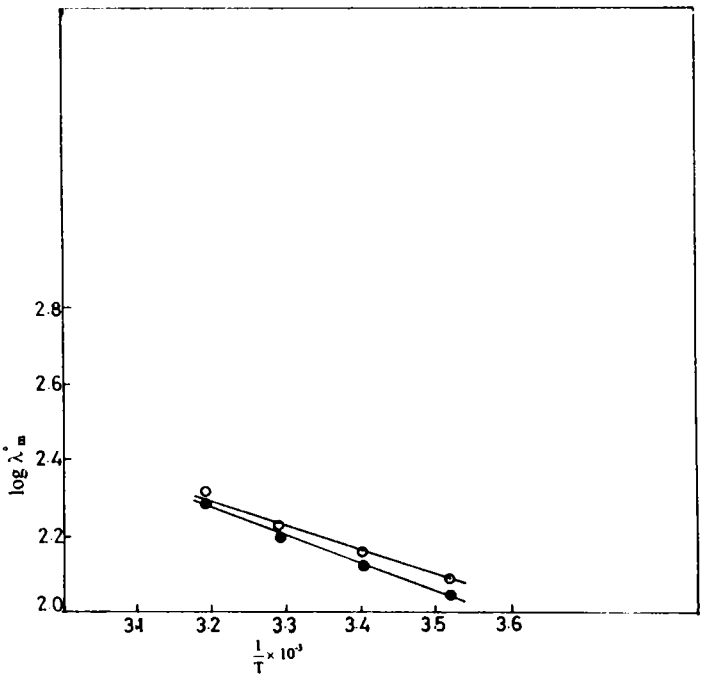

Figure 7.2 Plot of $\log \lambda^{\circ}_{m}$ vs $\frac{1}{T}$ for manganese(II) complexes

o $[Mn(ATSC)_2SO_4]$ • $[Mn(BTSC)_2SO_4]$

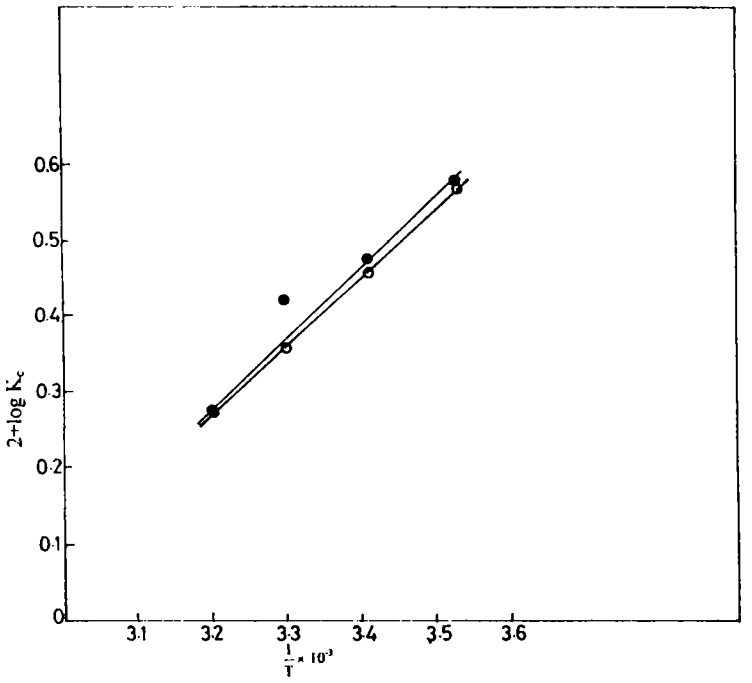

Figure 7.3 Plot of log K_c vs $\frac{1}{T}$ for manganese(II) complexes

o $[Mn(ATSC)_2SO_4]$ • $[Mn(BTSC)_2SO_4]$

Table7.3 Calculated values of R and R_s (in A°) for SO_4^{2-} ions at

Temperature	R	R_s
283K	2.29	3.26
293K	2.29	3.22
303K	2.29	3.18
313K	2.29	3.15

Table7. 4 Thermodynamic parameters of dissociation and ion-solvent interaction

	$Mn(ATSC)_2SO_4$				$Mn(BTSC)_2SO_4$			
	283 K	293 K	303 K	313 K	283 K	293 K	303 K	313 K
$\Delta H_{I\text{-}S}$ (Joule)	-220.90	- 223.20	-225.40	-227.40				
ΔG_D (kJ mol^{-1})	7.70	8.60	9.50	10.30	7.70	8.50	9.10	10.30
$\Delta G_{I\text{-}S}$ (Joule)	-224.40	-226.90	-229.40	-231.80				
$\Delta S_D \times 10^{-1}$ (kJ K^{-1} mol^{-1})	-93.00	-93.00	- 93.00	-92.00	-99.00	-98.00	-96.00	-97.00
$\Delta S_{I\text{-}S} \times 10^{-1}$ (Joule)	12.05	12.75	13.45	14.23				

temperature. ΔS_D is almost constant, small enough, and negative indicating the process of electrostriction or slight disorder in the process, perhaps this favours the association process proposed earlier. Entropy is significantly connected to the solvent structure perturbation brought about by the disordered ions. This small negative ΔS_D has been considered as due to increased orientation of water molecules and the formation of solvent separated or solvent shared ion-pairs.

The change in enthalpy ($\Delta H_{I\text{-}S}$), free energy ($\Delta G_{I\text{-}S}$) and entropy ($\Delta S_{I\text{-}S}$) of ion (SO_4^{2-}) solvent interaction at different temperatures using the following three equations proposed by Born [139].

$$\Delta G_{I\text{-}S} = -\frac{N_A (z_i e_o)^2}{2r_i} (1\text{-}1/\varepsilon) \qquad (9)$$

$$\Delta S_{I\text{-}S} = \frac{N_A (z_i e_o)^2}{2r_i} 1/\varepsilon^2 \, \delta\varepsilon/\delta T \qquad (10)$$

$$\Delta H_{I\text{-}S} = \Delta G_{I\text{-}S} + T \, \Delta S_{I\text{-}S} \qquad (11)$$

where z_i is the valency of cation and anion, e electronic charge, r corrected radius of the species (Table7.3), ε is the dielectric constant of the medium and $\delta\varepsilon/\delta T$ is the temperature coefficient.

In general these may be called as activation parameters of solvation process. The computed values of above three parameters of solvation for sulfate are shown in Table 7.4 at different temperatures. Since SO_4^{2-} is the common species for both these complexes, activation parameters are also common for both the complexes. Solvation process is exothermic which is supported by the

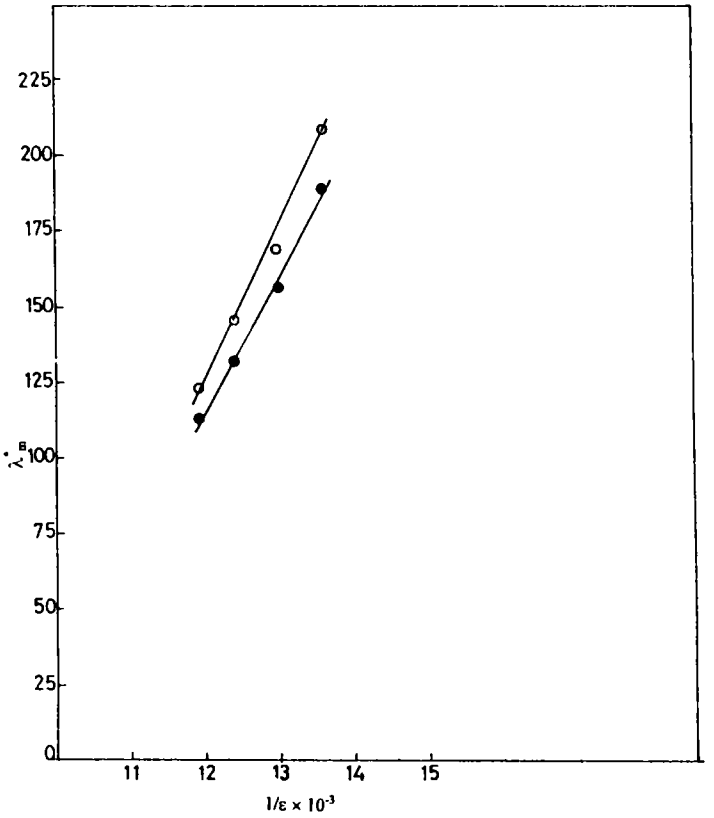

Figure 7.4 Plot of λ^{c}_{m} vs $1/\varepsilon$ for manganese(II) complexes

o $[Mn(ATSC)_2SO_4]$ • $[Mn(BTSC)_2SO_4]$

change in free energy which is spontaneous (negative). So the species tries to be in the solvated state according to Born. A plot of $\Delta G_{I\text{-}S}$ vs $1/R_s$ is drawn and found to be linear (Figure not shown) which propose the validity of Born equation to the process. Plot of λ°_{m} vs $1/\varepsilon$ is linear and shown in Figure 7.4. Entropy of ion-solvation is small, so small that, virtually no difference between $\Delta G_{I\text{-}S}$ and $\Delta H_{I\text{-}S}$ which is in confirmity with the proposal made by Elay and Evans [139].

7.3.5 Walden product

The walden product [139 - 143], which is the product of viscosity of the solvent and the limiting conductance, was calculated and presented in Table 7.5. The values are found to slightly decrease with increase in temperature indicating the increase of Stoke's molecular radius. To prove this the Stoke's molecular radius was calculated and shown in Table 7.5. The radius found to increase with increase in temperature as proposed. This increase in radius hints at the increased ion-solvent interaction. That means ions are more solvated at this temperatures which is on expected trend (hydration number of sulfate is around 8) so the role of sulfate in deciding about limiting molar conductance is very little. Only the cation moiety is responsible for the observed variation in conductance. It is likely that hydrated cationic moiety has undergone little association and this association must be a solvent separated or solvent shared ion-pair as both cation and anion of the complex are hydrated to large extent. Since the limiting conductance is continuously increasing with increase of temperature, it may also be expected that there may be some charged ion pairs and ion triplets [136]. Because of these, the molecular size slightly increases with the increase in temperature, at the same time limiting conductance also increases. This is in tune with the proposal made in the case of increase of association constant with increase of temperature. The increase in conductance is not nullified by the decrease in viscosity of the solvent as expected.

Table 7.5 Computed walden product (λ°_m ohm^{-1} cm^2 mol^{-1} poise) and Stoke's molecular radius (r : 10^{-8}cm) for two complexes at 283, 293, 303 and 313 K.

Temperature	$Mn(ATSC)_2SO_4$		$Mn(BTSC)_2SO_4$	
	Walden product	Stoke's radius	Walden product	Stoke's radius
283 K	1.60	1.00	1.40	1.10
293 K	1.50	1.10	1.30	1.20
303 K	1.30	1.20	1.20	1.30
313 K	1.20	1.30	1.10	1.40

Table 7.6 Computed transport number and limiting molar conductance of $Mn(ATSC)_2SO_4$ and $Mn(BTSC)_2SO_4$ at

Temperature	$Mn(ATSC)_2SO_4$		λ°_m of $[Mn(ATSC)_2]^{2+}$	λ°_m of SO_4^{2-}	$Mn(BTSC)_2SO_4$		λ°_m of $[Mn(BTSC)]_2^{2+}$
	t_+	t_-			t_+	t_-	
283 K	0.56	0.44	69.01	54.99	0.51	0.49	56.12
293 K	0.51	0.49	75.51	71.49	0.46	0.54	60.09
303 K	0.46	0.54	77.30	89.37	0.43	0.57	66.88
313 K	0.43	0.57	89.17	119.16	0.38	0.62	73.15

SUMMARY

The thesis deals with the synthesis, characterization, electrochemical and biological studies of transition metal complexes of two salicylaldehyde ^4N-monosubstituted thiosemicarbazones, *viz.* salicylaldehyde ^4N-phenylthiosemicarbazone and salicylaldehyde ^4N-cyclohexylthiosemicarbazone.

The thesis is divided into seven chapters. Chapter I of the thesis presents an introduction about metal complexes of thiosemicarbazones. Bonding, stereochemistry, biological and analytical applications of transition metal complexes of thiosemicarbazones and objective and scope of the present work are also outlined in this chapter.

Chapter II contains informations on synthesis, purification and characterization of the ligands by IR, ^{1}H and ^{13}C NMR and physico-chemical techniques employed in the characterization of metal complexes.

Chapter III deals with the synthesis and characterization of heterocyclic base adducts of copper(II) complexes of salicylaldehyde ^4N-phenyl- and ^4N-cyclohexyl-thiosemicarbazone. IR, electronic and EPR spectra of the complexes have been obtained. Based on EPR studies all possible parameters have been calculated. The g values, calculated for all the complexes in frozen solution indicate the presence of the unpaired electron in the $d_{x^2-y^2}$ orbital. The metal-ligand bonding parameters evaluated showed strong in-plane σ and in-plane π bonding. The magnetic and spectroscopic data indicate a square planar geometry for the four-coordinate and a distorted square pyramidal for five-coordinate complexes. From cyclic voltammetric data quasireversible copper(II)/copper(I) couples are observed for all the complexes except CuL^1phen, which is irreversible. Salicylaldehyde ^4N-phenylthiosemicarbazone and its copper(II) complexes have been tested against human pathogenic bacteria and plant pathogenic fungi. All the complexes exhibit antibacterial and antifungal activities.

Chapter IV contains the synthesis and characterization of heterocyclic base adducts of nickel(II) complexes of salicylaldehyde ^4N-phenyl- and ^4N-cyclohexyl-thiosemicarbazone. Four-coordinate complexes, py, pip and NiL^2 are diamagnetic and square planar, β/γ-pic complexes exhibit square planar ⇌ tetrahedral equilibrium, imz complexes have tetrahedral structure and five-coordinate complexes, phen and dipy have pseudo-octahedral structure. Salicylaldehyde ^4N-cyclohexylthiosemicarbazone and its nickel(II) complexes are active against human pathogenic bacteria and plant pathogenic fungi.

Chapter V gives details about the synthesis an characterization of cobalt(II) complexes of salicylaldehyde ^4N-phenyl- and ^4N-cyclohexyl-thiosemicarbazone and heterocyclic bases. Square planar structure is assigned for four-coordinate py, pip and imz complexes and square pyramidal structure for five-coordinate phen and dipy complexes. Analysis of EPR spectra indicate the presence of unpaired electron in the d_{z^2} orbital.

Chapter VI includes the synthesis and characterization of one iron(III) complex.. IR, electronic and EPR spectra indicate a square pyramidal structure for this complex. Mössbauer spectrum reveals the presence of two high spin iron(III) species in this complex and the observed magnetic moment value is higher than that expected for a five-coordinate complex. Magnetic, EPR and Mössbauer studies reveal the existence of a quantum admixture of S = 3/2 and S = 5/2 states in this complex.

Chapter VII contains the conductometric studies of manganese(II) complexes of acetonethiosemicarbazone and butanonethiosemicarbazone in water at 283, 293, 303 and 313 K. The calculation of thermodynamic parameters gave a clear idea about the association of these complexes in water under the studied concentration range.

REFERENCES

1. M. Akbar Ali and S. E. Livingstone, *Coord. Chem. Rev.*, 1974, **13**, 101.

2. M.J. M. Campbell, *Coord. Chem. Rev.*, 1975, **15**, 279.

3. S. Padhye and G. B. Kauffman, *Coord. Chem. Rev.*, 1985, **63**, 127.

4. D. X. West, S. B. Padhye and P. B. Sonawane, *Structure and Bonding*, Springer Verlag, Heidelberg 1991, **76**, 1.

5. P. Domiano, G.G. Fava, M. Nardelli and P. Sgarabotto, *Acta Crystallogr.*, 1969, **25B**, 343; G. D. Andreto, P. Domiano, G.G. Fava, M. Nardelli and P.Sgarabotto, *Acta Crystallogr.*, 1970, **26B**, 1005.

6. N. V. Gerbeleu, N.D. Revenko and V.M. Leovac, *Russ. J. Inorg. Chem.*, 1977, **22**, 1009.

7. F. Tui, K.I. Turta and N.V. Gerbeleu, *Russ. J. Inorg. Chem.*, 1977, **22**, 1497.

8. D.X. West and D.L. Huffman, *Transition Met. Chem.*, 1989, **14**, 190.

9. D.X. West, P.M. Ahrweiler, G. Ertem, J.P. Scovill, D.L. Klayman, J.L. Flippen-Anderson, R. Gilaradi, C. George and L.K. Pannell, *Transition Met. Chem.*,1985, **10**, 264.

10. H.K. Parwana and G. Singh, *Indian J. Chem.*, 1987, **26A**, 591.

11. M.D. Timken, S.R. Wilson and D.N. Hendrickson, *Inorg. Chem.*, 1985, **24**, 3450.

12. D. X. West, R.M. Makeever, J.P. Scovill and D.L. Klayman, *Polyhedron*, 1984, **3**, 947.

13. P. Sonawane, R. Chikate, A. Kumbhar, S. Padhye and R.J. Doedens, *Polyhedron*, 1994, **13**, 395.

14. A.B. Ablov and N.V. Gerbeleu, *Russ. J. Inorg. Chem.*, 1964, **9**, 1260.

15. M. Mohan, P. Sharma, M. Kumar and N.K. Jha, *Inorg. Chim. Acta*, 1986, **9**, 125.

16. M. Mohan, A. Agarawal and N.K. Jha, *J. Inorg. Biochem.*, 1988, **34**, 41.

17. U.N. Shetti, V.K. Revankar and V.B. Mahale, *Proc. Indian Acad. Sci. (Chem.Sci.)*, 1997, **109**, 7.

18. D.X. West, J.S. Ives, G.A. Bain, A.E. Liberta, J. Valdes-martinez, K.H. Ebert, S. Hernandez-ortega, *Polyhedron*, 1997, **16**, 1895.

19. I. Atonini, F. Claudia, P. Franchetti, M. Grifantini and S. Martelli, *J. Med. Chem.*, 1977, **20**, 447.

20. I. Atonini, F. Claudia, P. Franchetti, M. Grifantini and S. Martelli, *Eur. J. Med.Chem*, 1977, **14**, 89; T.L. Lemke, T.W. Shek, L.A. Cates and L.K. Smith, *J.Med. Chem.*, 1977, **20**, 135; S.K. Khetan, *Chem. Ind.* (London), 1973, 183.

21. D.X. West, J.P. Scovill, J. Silverton and A. Bavoso, *Transition Met. Chem.*, 1986, **11**, 123.

22. B.S. Garg, M.R.P. Kurup, S.K. Jain and Y.K. Bhoon, *Transition Met. Chem.*, 1991, **16**, 111.

23. D.X. West, M.A. Lockwood, H. Gebremedhin, A. Castineiras and A.E. Liberta, *Polyhedron*, 1993, **12**, 1887.

24. D.X. West, H. Gebremedhin, R.J. Butcher, J.P. Jasinski and A.E. Liberta, *Polyhedron*, 1993, **12**, 2489.

25. D.X. West, A.C. Whyte, F.D. Sharif, H. Gebremedhin and A.E. Liberta, *Transition Met. Chem.*, 1993, **18**, 238.

26. R.J. Butcher and D.X. West, *Transition Met. Chem.*, 1993, **18**, 449.

27. D.X. West, S.L. Dietrich, I. Thientanavanich, C.A. Brown and A.E. Liberta, *Transition Met. Chem.*, 1994, **19**, 195.

28. D.X. West, H. Gebremedhin, T.J. Romack and A.E. Liberta, *Transition Met. Chem.*, 1994, **19**, 426.

29. D.X. West, C.E. Ooms, J.S. Saleda, H. Gebremedhin and A.E. Liberta, *Transition Met. Chem.*, 1994, **19**, 553.

30. D.X. West, J.S. Ives, J. Krejci, M.M. Salberg, T.L. Zumbahlen, G.A. Bain, A.E. Liberta, J. Valdes-martinez, S. Hernandez-ortiz and R.A. Toscano, *Polyhedron,* 1995, **14**, 2189.

31. D.X. West, H. Gebremedhin, R.J. Butcher and J.P. Jasinski, *Transition Met. Chem.*, 1995, **20**, 84.

32. C. Maichle, A. Castineiras, R. Carballo, H. Gebremedhin, M.A. Lockwood, C.E. Ooms, T.J. Romack and D.X. West, *Transition Met. Chem.*, 1995, **20**, 228.

33. D.X. West, I. Thientanavanich and A.E. Liberta, *Transition Met. Chem.*, 1995, **20**, 303.

34. N.T. Akinchan, D.X. West, Y.H. Yang, M.M. Salberg and T.L. Klein, *Transition Met. Chem.*, 1995, **20**, 481.

35. D.X. West, G.A. Bain, R.J. Butcher, J.P. Jasinski, Yu Li, R.Y. Pozdniakiv, J. Valdes-martinez, R.A. Toscano and S. Hernandez-ortega, *Polyhedron,* 1996, **15**, 665.

36. D.X. West, N.M. Kozub and G.A. Bain, *Transition Met. Chem.*, 1996, **21**, 52.

37. D.X. West, A.M. Stark, G.A. Bain and A.E. Liberta, *Transition Met. Chem.*, 1996, **21**, 289.

38. D.X. West, I.S. Billeh, G.A. Bain, J. Valdes-martinez, K.H. Ebert and S. Hernandez-ortega, *Transition Met. Chem.*, 1996, **21**, 573.

39. D.X. West, J.S. Ives, G.A. Bain, A.E. Liberta, J. Valdes-martinez, K.H. Ebert and S. Hernandez-ortega, *Polyhedron*, 1997, **16**, 1895.

40. S.K. Chattopadhyay, D. Chattopadhyay, T. Banerjee, R. Kuroda and S. Ghosh, *Polyhedron*, 1997, **16**, 1925.

41. M. Akbar Ali, D.A. Chowdhary and M. Nazimuddin, *Polyhedron*, 1984, **3**, 595.

42. M. Akbar Ali, M.H. Kabir, M. Nazimuddin and S.M.M.H. Majumder, *Indian J.Chem.*, 1988, **27A**, 1064.

43. P. Bindu, M.R.P. Kurup and T.R. Satyakeerty, *National Seminar on Metal ions in Biological Sciences*, Department of Chemistry, I.I.T. Madras, India, March 1997.

44. M. Nazimuddin, M. Akbar Ali and F.E. Smith, *Polyhedron*, 1991, **10**, 1327.

45. M. Nazimuddin, M. Akbar Ali, F.E. Smith, and M.A. Mridha, *Transition Met. Chem.*, 1992, **17**, 74.

46. S.X. Liu, J.L. Tian, E.Q. Gao, S.W. Bi and Y.T. Li, *Syn. React. Inorg. Met.-Org.Chem.*, 1996, **26**, 1447.

47. R.B. Singh, B.S. Garg and R.P. Singh, *Talanta*, 1978, **25**, 619.

48. N.S.R. Reddy and D.V. Reddy, *Indian J. Chem.*, 1982, **21A**, 1076.

49. K. Hussain Reddy, Giridhara Reddy, K.M.M.S. Prakash and D.V. Reddy, *Indian J. Chem.*, 1984, **23A**, 535.

50. A.M.A. Khader and K.S. Prasad, *Turkish J. Chem.*, 1996, **20**, 222.

51. W.J. Geary, *Coord. Chem. Rev.*, 1971, **7**, 81.

52. M.H. El-Hammamy, A.A. Hasanein, S.A. El-Shazly and A.I. Kawana, *J. Electrochem. Soc. India*, 1987, **36**, 89.

53. Xu Shen, D. Wu, X. Huang, Q. Liu, Z. Huang and B. Kang, *Polyhedron*, 1997, **16**, 1477.

54. A. Berkessel, G. Hermann, O.T. Rauch, M. Buchner, A. Jacobi and G. Huttner, *Chem. Ber.*, 1996, **129**, 1421.

55. D.X. West, A.E. Liberta, S.B. Padhye, R.C. Chikate, P.B. Sonawane, A.S. Kumbhar and R.G. Yerande, *Coord. Chem. Rev.*, 1993, **123**, 49 and references therein; A.E. Liberta and D.X. West, *Biometals*, 1992, **5**, 121.

56. W.O. Foye, A.R. Banijamali and C.J. Patarapanich, *Pharm. Sci.*, 1986, **75**, 1180.

57. D. Ronen, L. Sherman, S. Nar-Nun and Y. Teitz, *Antimicrob. Agents Chemother.*, 1987, **31**, 1798.

58. D.L. Klayman, J.F. Bartosevich, T.S. Griffin, C.J. Mason and J.P. Scovill, *J. Med. Chem.*, 1979, **22**, 855.

59. D.E. Fenton, *Perspective in Coordination Chemistry*, (Eds. A.F. Wil, C. Floriani and A.E. Merbach) Verlag Helvitica Chimica Acta, Basel, 1992, 203.

60. E.I. Solomon, M.J. Baldwin and M.D. Lowery, *Chem. Rev.*, 1992, **92**, 521.

61. G.A. Bain, D.X. West, J. Krejici, J. Valdes-martinez, S. Hernandez-ortega and R.A. Toscano, *Polyhedron*, 1997, **16**, 855.

62. B. Harikumar, M.R.P. Kurup and T.N. Jayaprakash, *Transition Met. Chem.*, in press.

63. S.K. Jain, B.S. Garg, Y.K. Bhoon, D.L. Klayman and J.P. Scovill, *Spectrochim. Acta*, 1985, **41A**, 407.

64. D.X. West, C.S. Carlson, K.J. Bouck and A.E. Liberta, *Transition Met. Chem.*, 1991, **16**, 27.

65. B.S. Garg, M.R.P. Kurup, S.K. Jain and Y.K. Bhoon, *Transition Met. Chem.*, 1988, **13**, 309.

66. R.G. Inskeep, *J. Inorg. Nucl. Chem.*, 1962, **24**, 763.

67. A.A. Schilt and R.C. Taylor, *J. Inorg. Nucl. Chem.*, 1959, **9**, 217.

68. M. Manoyama, *Inorg. Chim. Acta*, 1975, **13**, 5.

69. M. Mikuria, H. Okawa and S. Kida, *Inorg. Chim. Acta*, 1979, **34**, 13; E. Ainscough, A.M. Brodie and N.G. Larsen, *Inorg. Chim. Acta*, 1982, **60**, 25.

70. M. Mikuria, H. Okawa and S.Kida, *Bull. Chem. Soc. Japan*, 1980, **53**, 3717.

71. B.B. Mahapatra and D. Panda, *Transition Met. Chem.*, 1979, **41**, 809.

72. M. Akbar Ali and S.G. Teoh, *J. Inorg. Nucl. Chem.*, 1979, **41**, 809.

73. L. Sacconi and G. Speroni, *J. Am. Chem. Soc.*, 1965, **87**, 3102; D.M.L. Goodgame, M. Goodgame and G.W. Rayner Canham, *J. Chem. Soc. A*, 1971, 1923.

74. J. Jezierska, *Asian J. Chem.*, 1992, **4**, 189.

75. A.H. Maki and B.R. McGarvey, *J. Chem. Phys.*, 1958, **29**, 35.

76. J.R. Wasson and C. Trapp, *J. Phys. Chem.*, 1969, **73**, 3763.

77. M.J. Bew, B.J. Hathaway and R.F. Faraday, *J. Chem. Soc. Dalton Trans.*, 1972, 1229.

78. B.N. Figgis, *Introduction to Ligand Fields*, (Interscience, New York) 1966, 295.

79. B.J. Hathaway, *Structure and Bonding*, 1973, **14**, 60.

80. S.H. Laurie, T-Lund and J.B. Raynor, *J. Chem. Soc. Dalton Trans.*, 1975, 1389.

81. M. Assour, *J. Chem. Phys.*, 1965, **43**, 2477.

82. A. Abragam and M.H.L. Pryce, *Proc. Roy. Soc.* (London), 1961, **A206**, 164.

83. A.M. Bond and R.L. Martin, *Coord. Chem. Rev.*, 1984, **54**, 23.

84. R.S. Nicholson, *Anal. Chem.*, 1965, **37**, 1351.

85. A.R. Hendrickson, R.L. Martin and N.M. Rhode, *Inorg. Chem.*, 1976, **15**, 2115.

86. B.J. Hathaway in G. Wilkinson, R.D. Gillard and J.A. McCleverty (Eds.) *Comprehensive Coordination Chemistry*, (Pergamon, Oxford) 1987, Vol **5**, 533.

87. G.S. Patterson and R.H. Holm, *J. Bioinorg. Chem.*, 1975, **4**, 1257.

88. A. Albert, C.W. Rees and A.J.H. Tmilson, *Rec. trav. Chim.*, 1956, **75**, 819.

89. D.E. Barber, Z. Lu, T. Richardson, R.H. Crabtree, *Inorg. Chem.*, 1992, **31**, 4709.

90. A.H. Vetter and A. Berkessel, *Synthesis*, 1995, 419.

91. R.H. Holm and M.J.O. Conner, *Prog. Inorg. Chem.*, 1971, **14**, 408.

92. J.C. Donini, B.R. Hellebone and A.B.P. Lever, *J. Am. Chem. Soc.*, 1971, **93**, 6455.

93. F.A. Cotton, *Progress in Inorganic Chemistry*, (Interscience, New York) 1964, Vol **6**.

94. J.S. Wood and P.T. Greene, *Inorg. Chem.*, 1969, **8**, 491.

95. S.L. Holt, R.J. Bouchard and R.L. Carlin, *J. Am. Chem. Soc.*, 1964, **86**, 519; D.H. Bush, *Adv. Chem. Ser.*, 1967, 616.

96. R.D. Bereman and G.D. Shields, *Inorg. Chem.*, 1979, **18**, 946.

97. S. Balasubramanian and C.N. Krishnan, *Polyhedron*, 1986, **5**, 669.

98. M.M. Mostafa, A. El-Hammid, M. Shallaby and A.A. El-Asmy, *Transition Met. Chem.*, 1981, **6**, 303.

99. K. Nakamoto, *Infrared and Raman Spectra of Inorganic and Coordination Compounds*, (Wiley Interscience, New York) 1986.

100. G.D. Hewkin and W.P. Griffith, *J. Chem. Soc. A*, 1966, 472.

101. A.B.P. Lever, *Inorganic Electronic Spectroscopy*, (Elsevier, Amsterdam) 1984.

102. M. Akbar Ali, S.E. Livingstone and D.J. Philips, *Inorg. Chim. Acta*, 1972, **6**, 39.

103. L.M. Thimmaiah, G.T. Chandrappa and W.D. Lloyd, *Inorg. Chim. Acta*, 1985, **107**, 281.

104. R.D. Jones, D.A. Summerville, F. Basolo, *Chem. Rev.*, 1979, **79**, 139.

105. T.D. Smith, J.R. Pilbrow, *Coord. Chem. Rev.*, 1981, **39**, 296.

106. C. Dual, C.W. Schlapfer, A.V. Zelewsky, *Structure and Bonding*, 1979, **36**, 129.

107. M.A. Hitchman, *Inorg. Chem.*, 1977, **16**, 1985.

108. K.S. Murray, A.V. Bergin, B.J. Kennedy and B.O. West, *Aust. J. Chem.*, 1986, **39**, 1479.

109. N. Herron, *Inorg. Chem.*, 1986, **25**, 4714.

110. S. Jayasree and K.K. Aravindakshan, *Polyhedron*, 1993, **12**, 1187.

111. A.A. El-Asmy and T.Y. Al-Asni, M. Mounir and S.A. Ashour, *Syn. React. Inorg. Met.-Org. Chem.*, 1989, **19**, 309.

112. A.A. El-Asmy, Y.M. Shaibi, I.M. Shedaiwa and M.A. Khattab, *Syn. React. Inorg. Met.-Org. Chem.*, 1990, **20**, 461.

113. P.S.K. Chia and S.E. Livingstone, *Aust. J. Chem.*, 1969, **22**, 1825 and references therein.

114. Rita Roy, Parimal Paul and Kamalaksha Nag, *Transition Met. Chem.*, 1984, **9**, 152.

115. R. Morassi, I. Bertini and L. Sacconi, *Coord. Chem. Rev.*, 1973, **11**, 343.

116. D.X. West, R.D. Profilet and J.L. Hines, *Transition Met. Chem.*, 1988, **13**, 467.

117. D.X. West and J.C. Severns, *Transition Met. Chem.*, 1988, **13**, 49.

118. B.S. Manhas, B.C. Verma and S. Balakrishna, *Polyhedron*, 1995, **14**, 3549.

119. O. Siimann and J. Fresco, *J. Am. Chem. Soc.*, 1970, **92**, 2652.

120. N.V. Gerbeleu, M.D. Revenko and V.G. Rusu, *Zh. Neorg. Khim.*, 1987, **32**, 946.

121. V.V. Zelentsov, G.I. Lapushkin, N.V. Gerbeleu, M.D. Revenko and V.G. Rusu, *Zh. Neorg. Khim.* 1987, **32**, 1651.

122. S.K. Jain, B. S. Garg and Y.K. Bhoon, *Transition Met. Chem.*, 1986, **11**, 89.

123. F.A. Cortton and G. Wilkinson, *Advanced Inorganic Chemistry*, (Wiley Interscience, New York) 1980, 761.

124. V.M. Leovac, L.J. Bjelica, L.S. Jovanovic and S.Yu. Chundak, *Polyhedron*, 1986, **5**, 983.

125. G.E. Chapps, S.W. McCann, H.H. Wickman and R.C. Sherwood, *J. Chem. Phys.*, 1974, **60**, 990.

126. T. Castner, G.S. Newell, W.C. Holton and C.P. Slichter, *J. Chem. Phys.*, 1960, **32**, 668.

127. H.H. Wickman, M.P. Klein and D.A. Shirley, *J. Chem. Phys.*, 1965, **42**, 2113.

128. M.C. Chan and J.O. Arkman, *Phys. Rev.*, 1969, **187**, 723.

129. N.N. Greenwood and T.C. Gibb, *Mössbauer Spectroscopy*, (Chapman and Hall Ltd. London) 1971.

130. M.M. Maltempo, *J. Chem. Phys.*, 1974, **61**, 2540.

131. S. Martin Nelson, *Comprehensive Coordination Chemistry*, (Pergamon, Oxford) 1987, Vol **5**, 217.

132. E. Yeager and A.J. Salkind, *Techniques of Electrochemistry*, 1973, Vol **2**.

133. J. Koryta and Dvorak, *Principles of Electrochemistry*, (John Wiley & sons, New York) 1987.

134. Sulekh Chandra and Yogendra Kumar, *Proc. Indian Acad. Sci. (Chem. Sci.)*, 1983, **92**, 249.

135. Kraus-Bray, *J. Am. Chem. Soc.*, 1913, **35**, 1337.

136. Y. Marcus, *Ion solvation*, (Wiley Interscience, New York) 1985.

137. B.E. Conway, *Ion Hydration in Chemistry and Biophysics*, (Elsevier scientific publishing company, New York) 1981.

138. L.P. Safoneva and A.M. Kolkar, *Russian Chem. Rev.*, 1992, **61**, 959.

139. J.O.M. Bockris and A.K.N. Reddy, *Modern Electrochemistry*, (Plenum press, New York) 1970, Vol **1**.

140. S.H. Maron and C.F. Prutton, *Principles of Physical Chemistry*, (Oxford & IBH, New Delhi) 1972.

141. J. Ishwara Bhat and P. Bindu, *J. Electrochem. Soc. India*, 1993, **42**, 103.

142. J. Ishwara Bhat and P. Bindu, *Pak. J. Sci. Ind. Res.*,1994, **37**, 313.

143. J. Ishwara Bhat and P. Bindu, *J. Indian Chem. Soc.*,1995, **72**, 783.

144. B.S. Kramgatz, *J. Chem. Soc. Faraday Trans. 1*, 1983, **79**, 571.

LIST OF RESEARCH PUBLICATIONS

A part of the contents of this thesis has been published/communicated for publication in the following form

1. **Studies on mixed ligand complexes of copper(II) with a substituted salicylaldehyde thiosemicarbazone**, M.R. Prathapachandra Kurup and P.Bindu, ***National Symposium on Current Trends in Coordination Chemistry***, March, 1995, Department of Applied Chemistry, Cochin University of Science and Technology, Kochi 682 022.

2. **Synthesis, Spectral characterization and Biological Activity of Cu(II) complexes containing Mixed Ligands**, P. Bindu, M.R. Prathapachandra Kurup and T.R. Satyakeerty, ***National Seminar on Metal ions in Biological Sciences***, March, 1997, Department of Chemistry, IIT Madras 600 036.

3. **ESR and Electrochemical Studies of four- and five-coordinate Copper(II) complexes containing mixed ligands**, P. Bindu and M.R. Prathapachandra Kurup, ***Transition Met. Chem*** (in press).

4. **Spectral studies of Nickel(II) complexes of an ONS donor ligand with Heterocyclic Bases**, P. Bindu and M.R. Prathapachandra Kurup, ***Indian J. Chem. Section A*** (in press).

5. **Conductometric Study of manganese(II) complexes of thiosemicarbazones as a function of Temperature**, P. Bindu, M.R. Prathapachandra Kurup and J. Ishwara Bhat, ***J. Electrochem. Soc. India*** (communicated).